

Alma Mater Studiorum – Università di Bologna

**DOTTORATO DI RICERCA IN
Biologia Cellulare e Molecolare**

Ciclo XXVI

Settore Concorsuale di afferenza: 05/E1

Settore Scientifico disciplinare: Bio/12

TITOLO TESI

*CELL DEATH MECHANISMS TRIGGERED BY MONOCLONAL ANTIBODIES
AGAINST CD99 IN EWING SARCOMA: CROSS-TALK BETWEEN MDM2, IGF-1R
AND RAS/MAPK*

Presentata da: **Terracciano Mario**

Coordinatore Dottorato

Chiar.mo Prof. Vincenzo Scarlato

Relatore

Chiar.ma Prof.ssa Michela Rugolo

Correlatore

Chiar.ma Prof.ssa Katia Scotlandi

Esame finale anno 2014

INDEX

INTRODUCTION.....	2
1. BONE SARCOMAS.....	2
2. EWING SARCOMA.....	3
2.1 Classification.....	3
2.2 Epidemiology and risk factors.....	3
2.3 Localization and histopathology.....	4
2.4 Course and therapies.....	5
2.5 Biology of Ewing sarcoma.....	6
3. CD99 ANTIGEN.....	9
3.1 MIC2 gene and CD99 protein.....	9
3.2 CD99 expression in normal and tumoral tissues.....	10
3.3 CD99 function.....	11
4. CELL DEATH MECHANISMS.....	12
4.1 Apoptosis and autophagy: the main types of programmed cell death.....	14
4.2 Macropinocytosis: an endocytic pathway leading to cell death.....	17
5. IGF SYSTEM.....	19
5.1 IGF-1 receptor (IGF-1R) and its molecular signaling.....	20
5.2 Ras proteins: structure and function.....	22
5.3 IGF system and cell death: a “paradoxical” role of Ras-MAPK pathway.....	23
PRELIMINARY DATA AND AIM OF THE STUDY.....	24
MATERIALS AND METHODS.....	28
RESULTS.....	34
1. IGF-1R/MDM2 relationship in ES.....	34
2. IGF-1R modulations following 0662 mAb treatments.....	34

3. CD99 internalization after its recruitment by 0662 mAb.....	36
4. CD99 stability.....	38
5. Role of lysosomes and endosomes in CD99 internalization process.....	40
6. CD99 internalizes both in a clathrin- and caveolin-1-dependent manner.....	42
7. CD99 and IGF-1R interaction upon 0662 treatment.....	44
8. IGF-1R is not degraded by 0662 mAb treatments.....	45
9. Ras-MAPK signaling is activated in response to treatment.....	48
10. Cytoplasm vacuolization during 0662 mAb-induced cell death: autophagy hypothesis.....	51
11. Ras has an active role in the observed cell death.....	53
12. Mesenchymal stem cells are resistant to 0662 mAb-induced cell death.....	55
13. EWS/FLI1 favors the delivering of the CD99-induced cell death message.....	57
DISCUSSION.....	59
REFERENCES.....	64

INTRODUCTION

1. BONE SARCOMAS

Bone sarcomas represent an heterogeneous class of malignant tumors of different connective tissues like bones, muscles and cartilage. Global incidence is around 5 new cases/100000 inhabitants/year, in particular 3000 new cases/year are reported in Great Britain and Italy and about 12000 new cases in USA. This incidence is considered 1/5-1/6 of all sarcomas, with osteosarcomas the most frequent (0.2 new cases/100000 inhabitants/year) followed by the Ewing family tumors with an incidence considered one-half in comparison to osteosarcomas. In the past years the great heterogeneity of sarcomas made diagnoses complicated and targeted therapeutic regimes very difficult to be performed; recently, the development of much more accurated methodologies allowed to get a molecular profile – based classification that divides sarcomas into two big groups: the first one, which includes alveolar rhabdomyosarcoma, synovial sarcoma and Ewing Sarcoma, is characterized by a simple cariotype with rare chromosomal rearrangements; the second one, comprising osteosarcoma and chondrosarcoma, is associated to a complex cariotype with numerous genetic alterations. These alterations involve oncosuppressor genes, like p53 and Rb, which can lead to aneuploidy or chromosomal aberrations of different nature, while the ones with simple cariotype are usually characterized by specific chromosomal traslocations able to generate chimeric proteins with deregulated activity. Frequently the mutated genes code for transcription factors or signal molecules involved in proliferation mechanisms like growth factors and/or their

receptors and, following mutations, they show crucial alterations of regulatory or functional motives like DNA binding domains (1).

2. EWING SARCOMA

2.1 Classification

Ewing sarcoma (ES) is a very rare and aggressive bone tumor of mesenchymal origin (2) described for the first time by James Ewing as a “diffuse endothelioma of bone” and later as an “endothelial myeloma of bone”. Because of its highly undifferentiated small round cell phenotype, for many years it has been considered mainly an histologic diagnosis of exclusion. Nowadays, based on the identification of a common genetic lesion, a similar clinical behavior and response to treatment, the World Health Organization considers this type of tumor, Askin tumors, peripheral primitive neuroectodermal tumor (PNET) and extraosseous ES belonging to the *Ewing sarcoma family tumors (ESFT)*(3).

2.2 Epidemiology and risk factors

ES is the second most common bone tumor after osteosarcoma, it usually strikes children and young adults with a peak of incidence between 10 and 20 years of age(4) and with a slight prevalence of males than females (1,5:1). Moreover, for unknown reasons, Ewing tumors occur most often in whites (either non-Hispanic or Hispanic), they are less common among Asian Americans and are extremely rare among African Americans. Despite the plethora of data reporting neuroectodermic and stomach cancers in families of patients with ES(5), there are no evidences highlighting an association between this type of tumor and congenital or family syndrome, while it seems to arise as a second tumor in patients previously subjected to radiotherapy, although with a lesser extent if compared to osteosarcoma. Lifestyle-related risk

factors such as body weight, physical activity, diet, and tobacco use play a major role in many adult cancers, but they usually take many years to influence cancer risk, and they are not thought to be critical in childhood cancers, including Ewing tumors, for whom risk factors are still obscure.

2.3 Localization and histopathology

The tumor onset may affect flat, short or long bones and it is very rare in the skull. The most common localization in the appendicular skeleton is the femur, followed by the tibia, humerus, fibula and forearm bones, while in the trunk the pelvis is the most frequent site of occurrence, followed by vertebrae and scapula, ribs and clavicle.

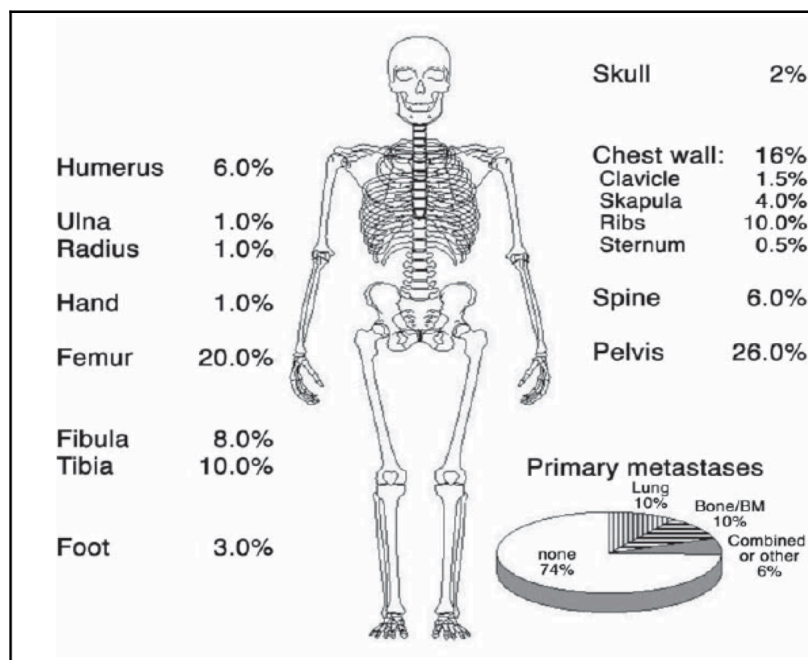


Figure 1. Ewing sarcoma localizations (4)

Microscopically this cancer is characterized by sheets of small rounded cells closely packed, without matrix and rich in glycogen: the cytoplasm is scarce, pale, granular and with poorly defined limits; nuclei, on the other hand, present a distinct nuclear membrane and they represent the bigger part of the cell.

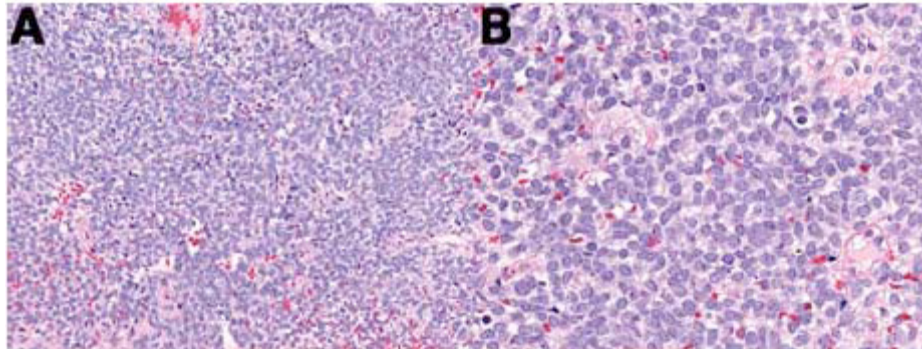


Figure 2. Histology of Ewing sarcoma/PNET (4)

2.4 Course and therapies

This type of sarcoma usually displays an aggressive growth with a multiple metastatic spread to the lungs, skeleton, lymph nodes and brain, a feature that used to make the long-term survival less than 10% before the employment of chemotherapy. Nowadays, thanks to multimodal treatments, this percentage increased, making a 5-years survival possible without any recurrence in almost 60% of cases; nevertheless, if metastases are present at the time of diagnosis (20% of cases), the survival possibilities decrease dramatically to 20%. ES is sensitive to chemotherapy and radiotherapy, but surgery plays a fundamental role in treatment of the primary tumor, since it represents the best way to control the neoplasia locally and, in some cases, it allows to avoid radiotherapy. The preferred therapeutic approach includes chemotherapy given pre- and post-operatively, surgery (whenever feasible) and radiotherapy (together with surgery or as an alternative). The most effective drugs are cyclophosphamide, ifosfamide, adriamycin, vincristin, actinomycin D and etoposide;

multicentric clinical studies demonstrated a higher efficacy for the association of 4 drugs (vincristin, cyclophosphamide, adriamycin and actinomycin D) if compared to an association of 3 drugs or to the utilization of the single drugs alone. Patients with metastases at the time of diagnosis treated with the same therapeutic regimen utilized for patients having a localized tumor showed a worst prognosis. For these cases, promising results have been reached using a much more aggressive chemotherapy, with increased doses and the time between cycles of treatment reduced, followed by a bone marrow transplantation with a reinfusion of peripheral stem cells. Bone sarcomas are high grade tumors with a devastating tendency to metastatize; introduction of multidrug chemotherapy improved prognosis but the price is long-lasting treatments with very high toxicity and side effects. In addition, despite the plethora of recently developed new drugs, patients with metastasis and recurrent diseases still have a very poor prognosis due to the lack of effective novel therapies against these types of tumors. Further improvements obviously require advances in the biological and molecular understanding of these cancers.

2.5 Biology of Ewing sarcoma

Routinely, for ES diagnosis, in addition to the utilization of histochemical and immunohistochemical reactions to test different biological markers expression (Table 1), it is common the employment of electronic microscopy, cytogenetics and molecular biology techniques to identify the two main markers of Ewing sarcoma: the membrane glycoprotein p30/32MIC2, also known as CD99, and the chromosomal traslocation responsible for the generation of a chimeric protein, EWS-Ets, obtained as a result from the fusion of N-terminal portion of EWS protein to the C-terminal portion of a member of Ets family of trascription factors (2).

MARKERS IMMUNOHISTOCHEMISTRY	
▪ VIM	+
▪ CD99	+
▪ Caveolina-1	+
▪ Fli1	+
▪ CAM 5.2	+/-
▪ S100	+/-
▪ LAC	-
▪ TdT	-

Table 1. Markers routinely used with immunohistochemistry for ESFT diagnosis.

EWS gene is a member of TET transcription factors family, characterized by the presence of an 87 aminoacids region (RRM/RNP-CS) able to promote the RNA binding, and a glutamine-rich N-terminal portion involved in the fusion process to EST genes in ESFT tumors. EWS protein function is still poorly defined, even if it seems to be involved in trascription mechanisms since it was seen to be associated to RNA-polimerase subunits and products. Protein members of Ets family are transcription factors whose role can be to activate or downregulate the transcription, depending on their interaction with DNA and/or other regulatory proteins. DNA binding domain of Ets proteins is part of the chimeric product EWS-Ets, causing its aberrant trascriptional activity.

The traslocation t(11;22)(q24;q12) is present in almost 90% of ES cases; it causes the formation of EWS-FLI1 chimeric product, which is the main patognomonic alteration of ES, and it is characterized by binding of exon 7 of EWS gene to exon 5 (fusion type II) or 6 (fusion type I) of FLI1 gene (Figure 3). The chromosomal traslocation t(21;22)(q22;q12) responsible of EWS-ERG transcript generation is present in around

5% of the cases, while other chromosomal traslocations are much more rare (Table 2).

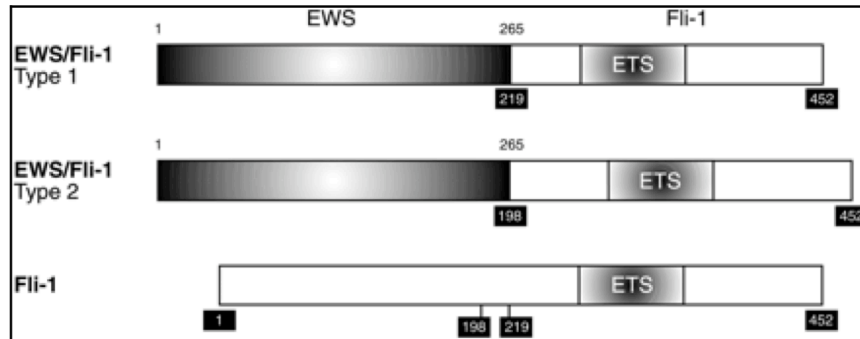


Figure 3. Different types of EWS/Fli-1 chimera (6)

TRASLOCATION	GENES	FREQUENCY
t(11;22)(q24;q12)	EWS-FLI1	90-95%
t(21;22)(q22;q12)	EWS-ERG	5-10%
t(2;22)(q33;q12)	EWS-FEV	Rare
t(7;22)(q22;q12)	EWS-ETV1	Rare
t(17;22)(q12;q12)	EWS-E1AF	Rare
t(2;16)	FUS-FEV	Rare
t(21;16)	FUS-ERG	Rare

Table 2. Genetic rearrangements typically involved in ESFT

EWS-FLI1 protein activity is necessary not only for cell transformation, as demonstrated by its forced expression in immortalized murine NIH3T3 fibroblasts (7), but also for the maintenance of the disease: silencing EWS-FLI1 leads to a

decrease in tumoral growth *in vivo* and *in vitro*(8, 9). Besides, numerous genes involved in the regulation of proliferation and tumorigenicity are also EWS-FLI1 specific targets: E2-C, among these, regulates stromelysin, a metallo-protease involved in migration and invasion processes, and C-MYC, a transcription factor known to have a role in proliferation and apoptosis. However, effects of EWS-FLI1 expression are strongly dependent on cellular background; critical factors in the permissive background are largely unknown, but may include the presence of an intact IGF pathway as well as of CD99, both of them very attractive from a therapeutic point of view since the first one is known to be upregulated through an autocrine activation in most of ES cases, and the second one is a membrane glycoprotein highly expressed in this type of tumor, a feature that makes it also a good diagnostic marker for ES.

3. CD99 ANTIGEN

3.1 MIC2 gene and CD99 protein

The membrane glycoprotein CD99 has been described for the first time in 1979 as an antigen particularly expressed in Acute Lymphoblastic Leukemia cells, being recognised by 12E7 monoclonal antibody (10).

It is coded by MIC2, a 50 kb gene mapping in the pseudo-autosomic region of both sexual chromosomes, X (Xp22.33-Xpter) and Y (Yp11-Ypter). Like all genes mapping in this region, MIC2 is characterized by interesting properties: the locus present on X chromosome does not undergo lyonization, allowing an equal distribution of MIC2 in males and females; besides, it does not follow the rules of sex-linked inheritance, and it segregates like autosomic alleles (11).

Particularly, MIC2 codes for two protein isoforms, resulting from an alternative splicing of the primary transcript, known as CD99 type I or wild type and CD99 type

II. Comparative gene sequence analyses revealed that cDNA of CD99 type II has a 18bp insert between the exon 8 and the exon 9 which is not present in the other isoform. Albeit its larger size, it codes for a truncated form of protein, since the 18bp insert introduces an in-frame stop codon responsible for the production of a 160 aminoacids instead of 185. Moreover, biochemical studies showed that CD99 undergoes post-translational modifications, like O-glycosylation, causing a reduction in protein molecular weight from 32 kDa to 28 kDa and 18 kDa (12).

To date a CD99 crystal structure is still missing because of its heavy glycosylation, but the use of cDNA sequence analyses gave us some indications: CD99 structure is made by an O-glycosylated extracellular domain of 100 aminoacids at the N-terminal portion, a putative hydrophobic transmembrane domain of 25 residues and a cytosolic C-terminal portion of 38 aminoacids, making possible the immunolocalization of the protein on the cellular surface (13-15). In order to have more information regarding the CD99 structure, circular dichroism and NMR spectroscopy analyses have been performed; these studies showed that the cytoplasmic portion of CD99 is characterized by the presence of an hairpin anchored to the plasma membrane with two flexible loops; for this reason, CD99 doesn't seem to have a regular secondary structure. It has been postulated that CD99 could gain a rigid conformation only when associated to other partners (16).

2.2 CD99 expression in normal and tumoral tissues

Immunohistochemical studies revealed a ubiquitous distribution of CD99 antigen, showing a high expression level in particular in ependymal cells of brain and bone marrow, in pancreatic islet, in Sertoli and Leyding cells, and in endothelial cells of blood vessels(17). The CD99 function in these cellular contexts is basically unknown, on the contrary, its role in hematopoietic system is well documented.

CD99 is differently expressed according to the cell type and differentiation stage (18-20). Particularly, CD34+ progenitor cells of bone marrow hematopoietic tissue

display high levels of CD99 antigen, which tend to decrease progressively with the increasing of differentiation and maturation stage towards type B lymphocyte and granulocyte lineage. Regarding CD99 expression in T lymphocyte, it results highly expressed in immature thymocytes but its levels decrease proceeding throughout differentiation processes (18, 21).

CD99 resulted expressed also in numerous tumors like acute lymphoblastic leukemia (10), embrional rhabdomyosarcoma (17, 22, 23), synovial sarcoma (24), mesenchymal condrosarcoma (25, 26) and ependymal tumors (27). However, Ewing sarcoma and peripheral neuroectodermic tumors represent the the higher CD99-expressing neoplasms, making the receptor a reliable diagnostic marker for the cited tumors, together with the specific chromosomal traslocations(17, 23).

2.3 CD99 function

Because of its still unknown ligand and the absence of a crystal structure, CD99 functions in phisiological conditions are barely described. Moreover, the existence of two different isoforms makes its role even harder to define. Although present on the X chromosome, the CD99 gene does not undergo X inactivation, indicating that the molecule should be involved in crucial biological processes. Indeed, CD99 was proved to play a role in monocyte diapedesis, T cell adhesion, apoptosis and differentiation, HLA exposure and intracellular trafficking (14, 28-31). In pathology, CD99 is present on the cell surface of ES, acute lymphoblastic leukemia (ALL), thymic tumours, synovial sarcoma, haemangiopericytoma, meningioma and malignant glioma, in which it results in higher levels of invasiveness and lower rates of survival compared to normal brain (23, 24, 32-34). On the contrary, a lower expression of CD99 antigen has been found in Osteosarcoma, a cellular context where it plays an oncosuppressor role(35, 36). In ES, high levels of CD99 are maintained by EWS-FLI1 (37-41), the oncogenic driver of ES (2), and expression of CD99 is required to create the permissive conditions for EWS-FLI1 transformation

(40): CD99 knock-down, in fact, leads ES cells to a terminal neural differentiated phenotype with neurite outgrowth, increased expression of β -III tubulin and neural differentiation markers; moreover, it reduces their ability to form tumors and bone metastases when xenografted into immunodeficient mice and diminishes their tumorigenic characteristics *in vitro*. On the other hand, triggering of CD99 with some, but not all, murine antibodies was found to deliver a massive and rapid cell-death message both in leukemic and ES cells (42-44) and significantly inhibits tumor growth and metastasis formation (45). All together these findings point out a potential immunotherapy employment of CD99, since it is easily accessible, it is expressed in virtually all cases (46) and it has a role in the pathogenesis of the tumor.

4. CELL DEATH MECHANISMS

Cell death can be classified according to its morphological appearance (which may be apoptotic, necrotic, autophagic or associated with mitosis), enzymological criteria (with and without the involvement of nucleases or of distinct classes of proteases, such as caspases, calpains, cathepsins and transglutaminases), functional aspects (programmed or accidental, physiological or pathological) or immunological characteristics (immunogenic or non-immunogenic)(47). The field of cell death research, anyway, has continued its expansion, significant progress has been made and new putative cell death modalities have been described since 2005, when the Nomenclature Committee on Cell Death (NCCD) formulated the guidelines for the definition of the different type of cell deaths (48).

Dying cells are engaged in a process that is reversible until a first irreversible phase or ‘point-of-no-return’ is trespassed. It has been proposed that this step could be represented by massive caspase activation (49), loss of $\Delta\Psi_m$ (50), complete permeabilization of the mitochondrial outer membrane(51) or exposure of

phosphatidylserine (PS) residues that emit ‘eat me’ signals for normal neighboring cells. However, these parameters are also frequently present in the context of non-lethal processes and differentiation pathways, making the concept of “point-of-no-return” hard to be specifically defined.

In the absence of a clearly defined biochemical event that can be considered as the point-of-no-return, the NCCD proposes that a cell should be considered dead when any one of the following molecular or morphological criteria is met: (1) the cell has lost the integrity of its plasma membrane, as defined by the incorporation of vital dyes (e.g., PI) *in vitro*; (2) the cell, including its nucleus, has undergone complete fragmentation into discrete bodies (which are frequently referred to as ‘apoptotic bodies’); and/or (3) its corpse (or its fragments) has been engulfed by an adjacent cell *in vivo* (Table 3.)(52).

Definition	Notes	Methods of detection ³⁻⁵
<i>Molecular or morphological criteria to define dead cells</i>		
Loss of plasma membrane integrity	Plasma membrane has broken down, resulting in the loss of cell's identity	(IF) Microscopy and/or FACS to assess the exclusion of vital dyes, <i>in vitro</i>
Cell fragmentation	The cell (including its nucleus) has undergone complete fragmentation into discrete bodies (usually referred to as apoptotic bodies)	(IF) Microscopy FACS quantification of hypodiploid events (sub-G ₁ peak)
Engulfment by adjacent cells	The corpse or its fragments have been phagocytosed by neighboring cells	(IF) Microscopy FACS colocalization studies
<i>Proposed points-of-no return to define dying cells</i>		
Massive activation of caspases	Caspases execute the classic apoptotic program, yet in several instances, caspase-independent death occurs. Moreover, caspases are involved in non-lethal processes including differentiation and activation of cells	Immunoblotting FACS quantification by means of fluorogenic substrates or specific antibodies
$\Delta\Psi_m$ dissipation	Protracted $\Delta\Psi_m$ loss usually precedes MMP and cell death; however, transient dissipation is not always a lethal event	FACS quantification with $\Delta\Psi_m$ -sensitive probes Calcein-cobalt technique
MMP	Complete MMP results in the liberation of lethal catabolic enzymes or activators of such enzymes. Nonetheless, partial permeabilization may not necessarily lead to cell death	IF colocalization studies Immunoblotting after subcellular fractionation
PS exposure	PS exposure on the outer leaflet of the plasma membrane often is an early event of apoptosis, but may be reversible. PS exposure occurs also in T-cell activation, without cell death	FACS quantification of Annexin V binding
<i>Operative definition of cell death, in particular in cancer research</i>		
Loss of clonogenic survival	This method does not distinguish cell death from long-lasting or irreversible cell cycle arrest	Clonogenic assays

Abbreviations: $\Delta\Psi_m$, mitochondrial transmembrane permeabilization; FACS, fluorescence-activated cell sorter; IF, immunofluorescence; MMP, mitochondrial membrane permeabilization; PS, phosphatidylserine

Table 3. Cell death criteria and methods used for its detection(52).

4.1 Apoptosis and autophagy: the main types of programmed cell death

Generally, a cell demise is “programmed” whether is genetically controlled and apoptosis and macroautophagy (here referred as autophagy) are universally known as the two fundamental types of programmed cell death.

The term “apoptosis” was coined in 1972 (53), it is a Greek word literally meaning “leaves falling from the tree” and represents a set of genetic and biochemical pathways essential for development and maintenance of pluricellular organisms. In particular, it plays an important role in the organogenesis during embryo development, and is involved in regulating cellular homeostasis in adult.

Alterations of the apoptotic machinery can lead to severe tissue damages and pathologies like cancer, autoimmune diseases, cronic diseases like diabetes and neurodegenerations. This type of death classically occurs through rounding-up of the cell, retraction of pseudopodes, pyknosis (reduction of cellular volume), chromatin condensation, nuclear fragmentation, plasma membrane blebbing (but maintenance of its integrity until the final stages of the process) (52). Cytoplasm shrinkage and the plasma membrane blebbing represent the final steps of the entire mechanism, ending with the formation of vesicles called “apoptotic corps” which, thanks to the presence of molecules like phosphatitilserine on their surface, are recognized by specialized phagocytes responsible for their degradation.

Caspases play a fundamental role in the apoptotic process, since their activation mark the “point of no return”(54). They represent a cystein-protease family necessary for the execution of both pathways of programmed cell death. The first one, called “the intrinsic pathway”, is basicly controlled by an interplay between proapoptotic and antiapoptotic members of Bcl2 family with the involvement of mitochondria; initiators of the pathway include increased intracellular reactive oxygen species, radiation-induced DNA damage, exposition to chemotherapeutic agents and the deprivation of growth factors. These initiators ultimately lead to increased mitochondrial permeability, thereby promoting the release of proapoptotic proteins (cytochrome c) from the intermitochondrial membrane space into the cytosol (55,

56). Another of these proteins, diablo homologue (SMAC/DIABLO), antagonizes cytosolic inhibitors of proapoptosis proteins, thus allowing the activation of caspases and hence progression to apoptosis. Activated caspase 9 mobilize caspases 3, 6, and 7, proteases that herald demolition of the cell by cleaving numerous proteins and activating DNases. The extrinsic pathway exploits the binding of members of the tumor necrosis factor (TNF) super-family to cell-surface “death receptors,” members of the TNF receptor family. Ligation of these receptors initiates the formation of the multiprotein death-inducing signaling complex. Aggregation of this complex causes conformational changes in its components that trigger the catalytic activity of caspase 8, a central mediator of apoptosis, and the activation of the same effector caspases of the intrinsic pathway (Figura 4).

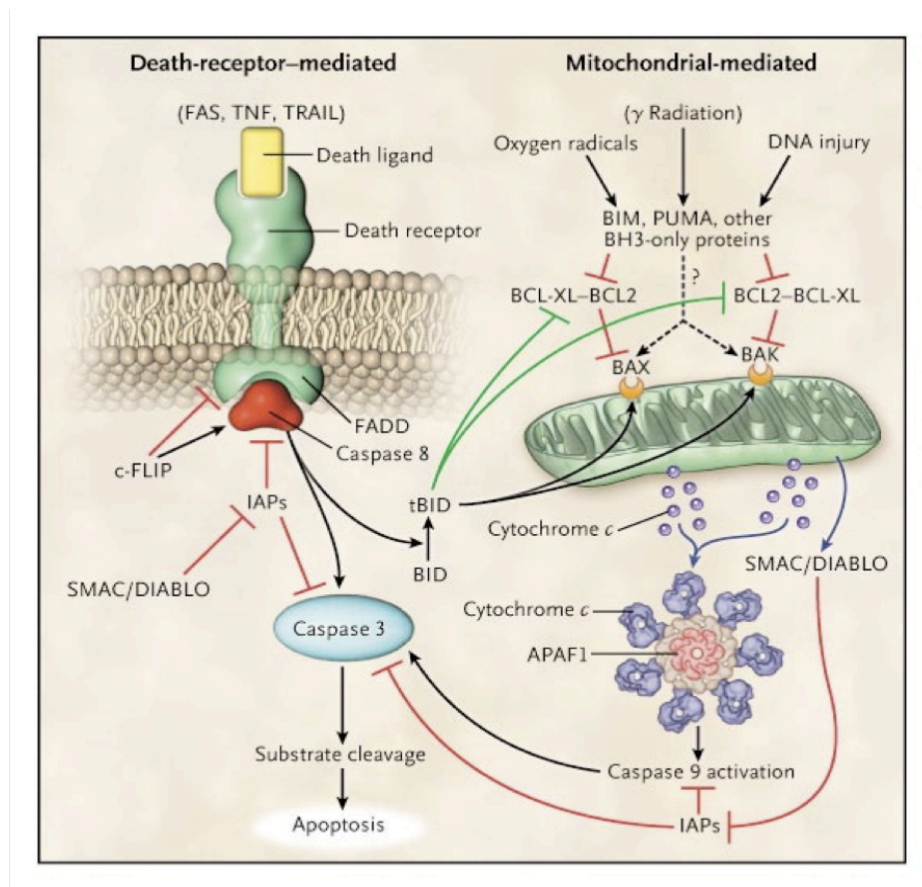


Figure 4. Schematic representation of the apoptotic process (57)

Autophagy is the process by which cells recycle their own redundant or damaged organelles and macromolecular components(58, 59). It is an adaptive response to sublethal stress, such as nutrient deprivation, that supplies the cell with metabolites it can use for fuel. Nevertheless, if prolonged, can compromise the cell viability and become an alternative cell death mechanism, leading the cell to self-digestion.

It is morphologically defined (especially by transmission electron microscopy) as a type of cell death that occurs in the absence of chromatin condensation but accompanied by massive autophagic vacuolization of the cytoplasm. In contrast to apoptotic cells (whose clearance is ensured by engulfment and lysosomal degradation), cells that die with an autophagic morphology have little or no association with phagocytes(60, 61).

This type of programmed cell death is characterized by the sequestration of cytoplasmic material within autophagosomes for bulk degradation by lysosomes. Autophagosomes, by definition, are two-membraned and contain degenerating cytoplasmic organelles or cytosol(62, 63). which allows them to be distinguished by transmission electron microscopy from other types of vesicles such as lysosomes or apoptotic blebs.

The autophagic process and machinery are complex, the former consists of five basic phases: initiation, elongation, closure, maturation, and degradation (Figure 5). The core machinery is constituted by different proteins and each of them has a relevant role within the stages of the process: the ATG1/unc-51-like kinase (ULK) complex, including ATG13 and the scaffold FIP200, and a second complex comprised of Vps34, a class III phosphatidylinositol-3-kinase (PI3K), and ATG6/Beclin1 (64) both regulate the initiation phases of autophagy. A third subgroup regulates later steps of autophagy, autophagosome elongation, and expansion, and is characterized by two ubiquitin-like proteins: LC3 (also known as ATG8/microtubule-associated protein 1 light chain 3) and ATG12 (65). LC3 becomes inserted into the inner and outer membranes of the autophagosome and has been used extensively to monitor autophagy. ATG12 is conjugated to ATG5 by the ATG7 and ATG10 proteins and

this ATG5– ATG12 conjugate interacts with ATG16L, promoting LC3 lipidation(66, 67). Autophagosomes, then, fuse with lysosomes, generating autolysosomes, in which both the autophagosome inner membrane and its luminal content are degraded by acidic lysosomal hydrolases. This catabolic process marks the completion of the autophagic pathway.

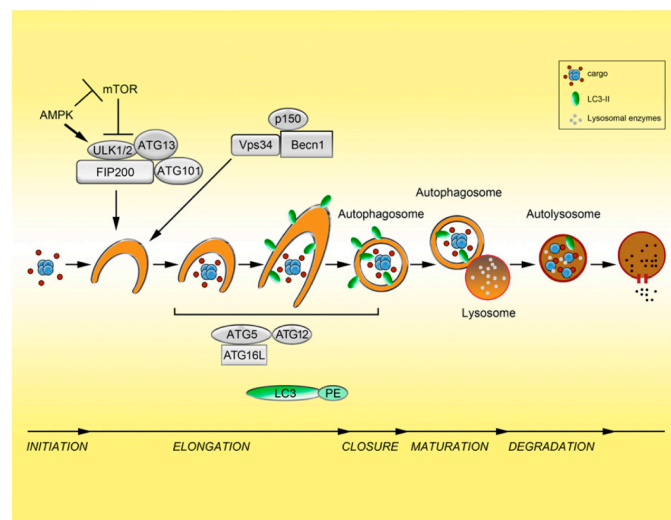


Figure 5. Proteins of the core machinery and autophagic process (68)

4.2 Macropinocytosis: an endocytic pathway leading to cell death

Apoptosis is the best characterized form of programmed cell death. However, during the last years nonapoptotic forms of cell death have been studied and recognized as playing significant roles during embryonic development, neurodegeneration, and cancer regression (69). In these cases, loss of cell viability may occur in a manner that is independent of caspase activation. In 1999, Chi et al.(70) reported that ectopic expression of activated Ras GTPase, which normally serves to stimulate cell proliferation, can trigger nonapoptotic cell death in glioblastoma and gastric carcinoma. This was described as autophagic death because the cells developed numerous cytoplasmic vacuoles. Later, in 2008, Overmeyer et al.(71) determined that

the large vacuoles observed in glioblastoma cells were derived from macropinosomes, terming this process “Methuosis” (from the Greek word *methuo*, which means “drink to intoxication”).

Macropinocytosis is a regulated form of endocytosis that mediates the uptake of solute molecules, nutrients and antigens in a clathrin-independent manner. It begins with an actin-mediated membrane ruffling of the plasma membrane, then some of the lamellipodia on the cell surface fold back onto themselves and fuse with the basal membrane creating large, irregular shaped vesicles termed *macropinosomes* which undergo a maturation process that is slightly different basing on the cellular context (Figure 6).

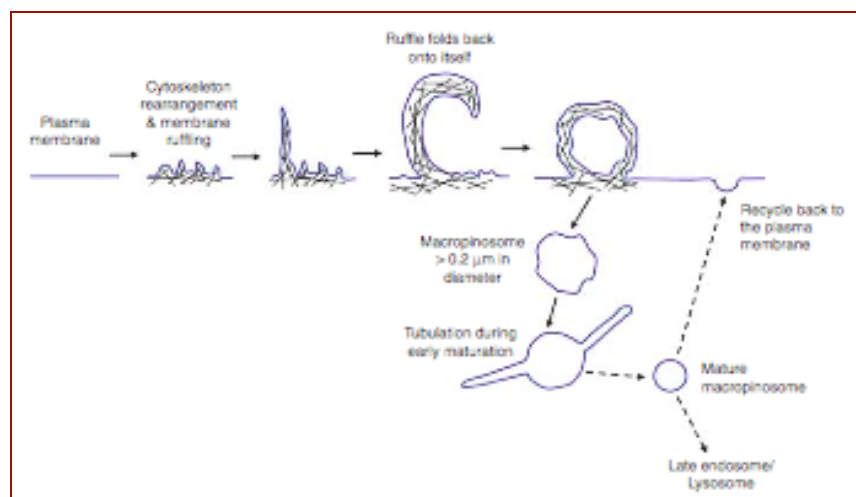


Figure 6. Pathway of Macropinocytosis (72)

This endocytic process has a physiological relevance: being associated with actin-dependent ruffling of the plasma membrane, this pathway is implicated in cell motility and, therefore, in tumor progression and metastasis; its role is also documented in the chemotactic response of neutrophils (73), while in the immune system, macropinocytosis is means by which cells internalize antigens to be then processed and loaded onto MHC molecules(74, 75). Although considerable progress has been made in understanding the cell biology of macropinocytosis, there remain

many unanswered questions: how do the different regulators of macropinocytosis regulate the entire process? Which events are associated with the formation and the maturation of macropinocytosis?

A key difference between clathrin-dependent endocytosis and macropinocytosis is that the latter requires actin cytoskeleton reorganisation. This was seen not only in *Dictyoselium discoideum* (76), but also in mouse macrophages (77), therefore, it does not surprise that components of signal transduction pathways linking receptor stimulation to actin cytoskeleton remodelling are also implicated as regulators of macropinocytosis. One such candidate is the Ras oncogene.

5. IGF SYSTEM

The role of growth factors in the pathogenesis of neoplasms is well documented, a lot of data in literature report a connection between tumors, growth factors and their own receptors. Among them, IGF system, being involved in cellular growth and proliferation because of its relevance in cell cycle progression from G1 to S phase, has been investigated by many research groups all around the world for years, disclosing its importance in developing and maintenance of different types of cancers. It is composed by several elements: two ligands IGF-1 and IGF-2; three membrane receptors IGF-1R, IGF-2R and IR; moreover, there are six proteins able to bind IGF ligands with a high affinity, IGF-Binding Proteins (IGFBP-1, -2, -3, -4, -5, -6), in order to modulate their bioavailability and preventing their degradation .

5.1 IGF-1 receptor (IGF-1R) and its molecular signaling

IGF-1R is a tetramer of 2 alpha and 2 beta chains linked by disulfide bonds; the alpha chains contribute to the formation of the ligand-binding domain, while the beta chain carries the kinase domain (78). Ligand binding (IGF-1 with a high affinity and IGF-2 with a lower affinity) activates the receptor kinase, leading to receptor autophosphorylation on tyrosines residues (Tyr-1165, Tyr-1161 and Tyr-1166) (79) and consequent phosphorylation of multiple substrates, that function as signaling adaptor proteins: the insulin-receptor substrates (IRSs proteins), Shc and 14-3-3 proteins. The IRS1 and Shc signaling pathways represent the main signal transmission routes regulated by IGF-1R, leading, respectively, to the induction of the PI3K-AKT/PKB pathway and the Ras-MAPK pathway (Figure 7). The recruitment of IRSs proteins on IGF-1R causes the phosphorylation of specific residues which act as docking sites for proteins SH2-containing domains, like PI3-K (phosphoinositide-3-kinase). In particular, they bind PI3-K regulatory subunit, p85, favoring the translocation of the catalytic subunit p110 on the plasma membrane, where, in turn, phosphorylates the phosphatidylinositol-(4,5)-biphosphate (PIP2) to phosphatidylinositol-(4,5)-triphosphate (PIP3). This event leads, ultimately, to the recruitment of B kinase protein (AKT) on the plasma membrane, with its subsequent conformational change and activation. AKT activation causes the induction of different proteins whose effect are the increase in protein synthesis mediated by mTOR on one hand, and on the other hand the apoptosis inhibition through the inhibitory phosphorylation of pro-apoptotic factors such as Bad. Shc activation stimulates, on the contrary, the Ras-MAPK pathway: Ras is a small membrane GTPase protein considered inactive if bound to GDP; following the receptor autophosphorylation, Sos factor (Son-of-sevenless) mediates the Ras activation catalyzing its binding with GTP. The association between Sos and its substrate is controlled by the adaptor protein Grb2, which is able to bind specific phosphotyrosines on the receptor and, in turn, is activated by interacting with Shc(80). Once in the active form, Ras translocates to the plasma membrane and

induces the activation of the serine/threonine kinase Raf; the latter is able to positively modulate the phosphorylation of a series of tyrosine-kinase proteins belonging to the MAP kinase family (Mitogen Activate Protein Kinase). All these events cause the Erk1/2 activation (Extracellular signal-regulated kinase), through the double phosphorylation borne by tyrosines and treonines residues. Erk, then, may phosphorylates different targets, both at the membrane or at the cytoplasmic level, besides, is also able to translocate into the nucleus and regulate the expression of specific transcription factors, such as Fos and Elk1.

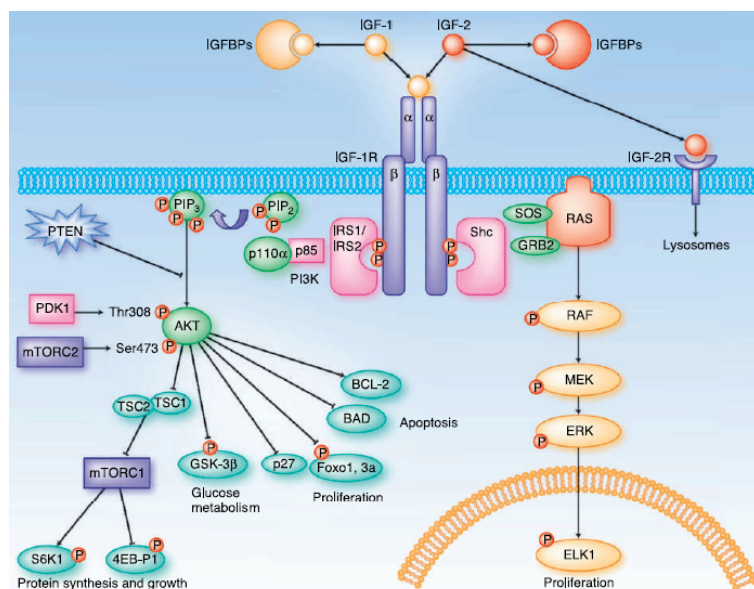


Figure 7. Key regulators of IGF-1R signal pathway (81)

5.2 Ras proteins: structure and function

Mammals encode three ras genes, H-ras, K-ras, and N-ras, whose protein product is present in every cell type and tissue although the expression pattern varies depending on the organ and the stage of development (82).

The product encoded by the ras genes is a protein of 188 amino acids (189 in KRasB) of approximately 21 kDa. The three isoforms show an homology in their first 164 amino acids, while they differ completely in the so called “heterogeneous region”, a segment of the carboxy-terminal region made by residues 165-185 (83). Ras biological activity resides in what has been termed the effector domain (amino acids 32 – 40) by means of which it binds to the different effector molecules (84).

Ras proteins exert their function switching from an inactive state, in which they are bound to guanine dinucleotides (GDPs), to an active state, bound to guanine trinucleotides (GTPs). This mechanism is tightly regulated by two types of regulatory proteins: guanine nucleotide exchange factors (GEFs), able to catalyze the GDP/GTP exchange, and GTPase- activating proteins (GAPs), which enhance the intrinsic capacity of Ras to hydrolyze GTP into GDP, thereby returning Ras to the inactive state (83, 85). Structural differences between the active and inactive states are apparently restricted to the switch I (residues 30 – 38) and switch II (residues 60 – 76) regions (86). The switch I region comprises the main binding site for effector molecules and GAPs, while the switch II region is involved in part in the interaction with GEF regions(84, 87, 88).

5.3 IGF system and cell death: a “paradoxical” role of Ras-MAPK pathway

Despite the foregoing, an increasing number of evidence demonstrate also a “paradoxical” role for IGF-1R and its effectors Ras-MAPK. In particular IGF-1R, among others, has been shown to be responsible of a nonapoptotic form of cell death in 293T cells called “paraptosis”, associated with a massive cytoplasmic vacuolization(90, 91); moreover, IGF-1R and IR have been found implicated in apoptotic mechanisms in primary cultured MEFs and in brown preadipocytes wheter the two receptors were both present and unoccupied (92). Despite its well described role in tumorigenesis as a pro-survival/proliferation factor, increasing evidence indicates that RAS is able to switch cell fate toward death in specific cellular contexts, such as in normal primary cells and in cancer cells under certain conditions(89, 93). Its activation can induce non-apoptotic cell death in neuroblastoma through a classical autophagic process (94, 95), while in glioblastoma RAS-regulated death occurs through Rac-dependent pathways hyperstimulating macropinocytosis (71). Depending on the duration, the magnitude and its subcellular localization, ERK activation controls various cell responses, such as proliferation, migration and differentiation but also death (96). A constitutive activation of ERK by active Raf (97), and IGF-I receptor(91) has been demonstrated to induce a form of cell death correlated with extensive cell rounding and the formation of cytoplasmic macrovacuoles, a morphology not related to an apoptotic cell death but that resembles rather an autophagic-like death or paraptosis. Moreover, depending on the cell type and the nature of the injury, ERK activation has been found associated both with the intrinsic apoptotic pathway(98-100) and with the extrinsic one (101-103). Notably, ERK promotes p53 stability and activity, a tumor suppressor involved also in apoptotic processes, by phosphorylating its serine 15 residue (104-106), and by inhibiting MDM2 phosphorylation on its serine 166 residue, which is associated with its ubiquitin ligase activity toward p53(107).

Preliminary data and aim of the study

Preliminary data demonstrate that CD99 triggering by monoclonal antibodies leads to a massive and rapid death of Ewing sarcoma cell lines *in vitro* and *in vivo*, through a non canonical caspase-independent mechanism (44). The employment of the anti-CD99 0662 antibody promotes, indeed, the phosphatidylserine exposure on the outer leaflet of the plasma membrane, a typical marker of the apoptotic process; nevertheless, the cell death occurs without caspases involvement or PARP clivage (Figure 9).

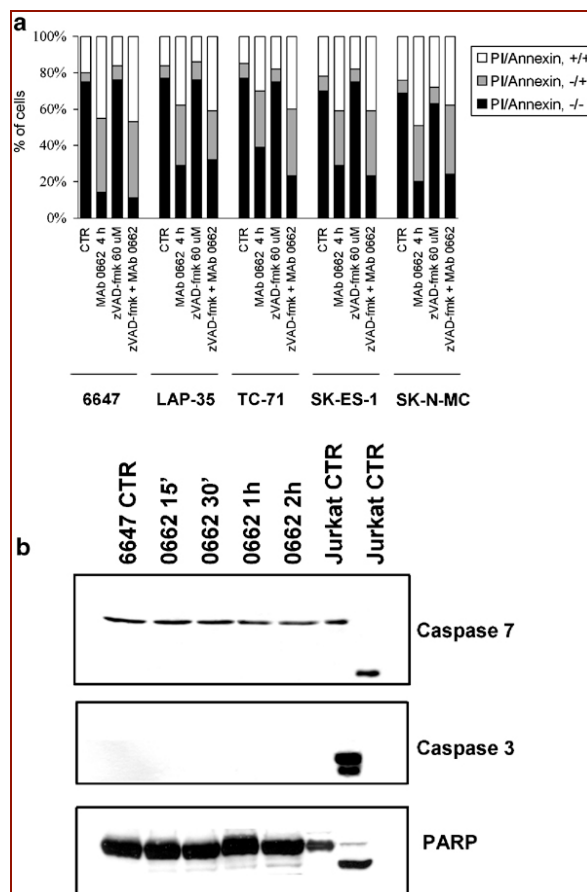


Figure 9. CD99-induced death occurs in a caspase-independent manner. (a). FACS analysis of Annexin V/PI in different ES cell lines following 0662 mAb treatments in presence or not of the caspase inhibitor zVAD-fmk. (b) Western blot analysis of caspase/PARP clivage in the ES cell line 6647(44).

The observed cell death mechanism is promoted by a reactivation of p53 through the phosphorylation on its serine 15 residue, an event that makes this transcription factor able to translocate into the nucleus, thus inducing the expression of some downstream effectors such as Bax and p21, the first one a pro-apoptotic factor and the second one a cell cycle inhibitor (Figure 10).

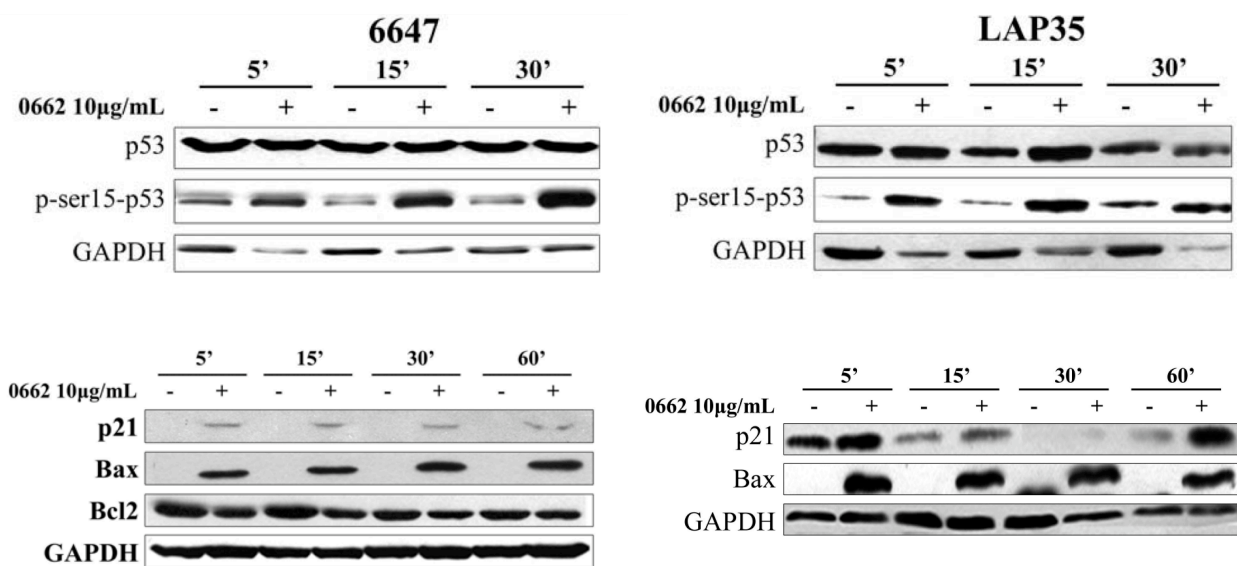


Figure 10. p53 phosphorylation and induction of its effectors p21 and Bax after 0662 mAb treatments in 6647 and LAP35 ES cell lines.

The fundamental role of p53 has been confirmed with *loss of function* experiments: exploiting siRNA oligonucleotides, p53 has been transiently knocked-down in 6647 and LAP35 cell lines, causing a reduction of the entire death mechanism if compared to the parental untransfected or scramble cell line, further suggesting that CD99-induced death is p53-dependent (Figure 11).

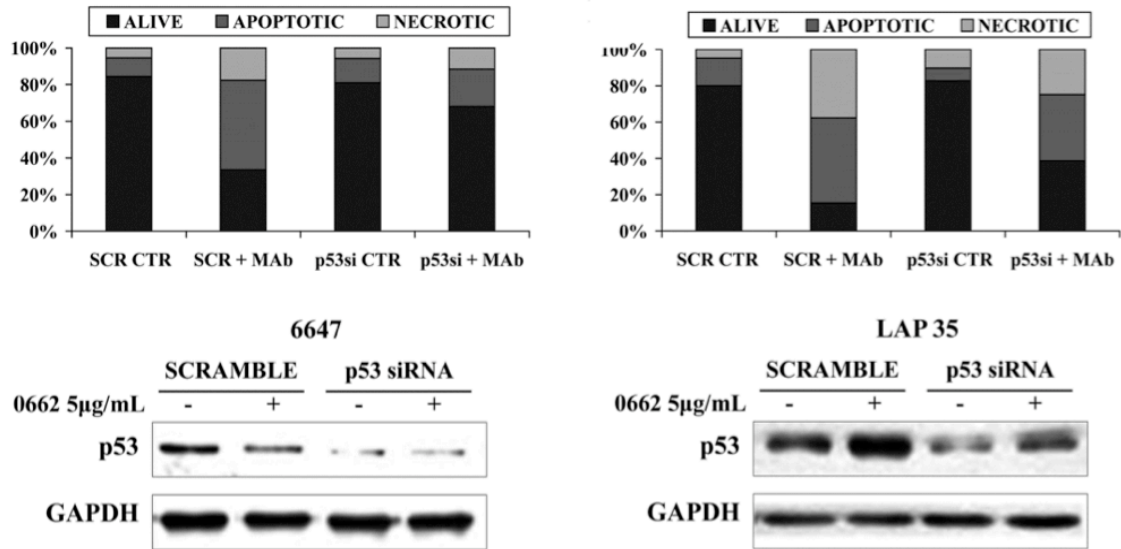


Figure 11. p53 participates actively to the CD99-induced cell death. In the upper panels Annexin V-PI analysis is shown, expressed as percentage of live (black), apoptotic (dark grey) or necrotic (light grey), in scramble or p53-silenced 6647 or LAP35 cells before and after treatment (30 min) with 5µg/mL 0662 MAb.

Normally, in non-transformed cellular contexts, p53 expression levels are regulated by MDM2, an E3 ubiquitin ligase which antagonizes the tumor suppressor by sequestering it into the cytoplasm, favouring, then, its ubiquitination and subsequent degradation by the proteasome. MDM2 is frequently overexpressed in ES (108), and our preliminary data demonstrate that its protein levels decrease in a time- and dose-dependent manner following 0662 mAb treatments, a reduction caused by a self-ubiquitination and proteasome degradation (Figure 12), leading, as a result, to the p53 reactivation previously described.

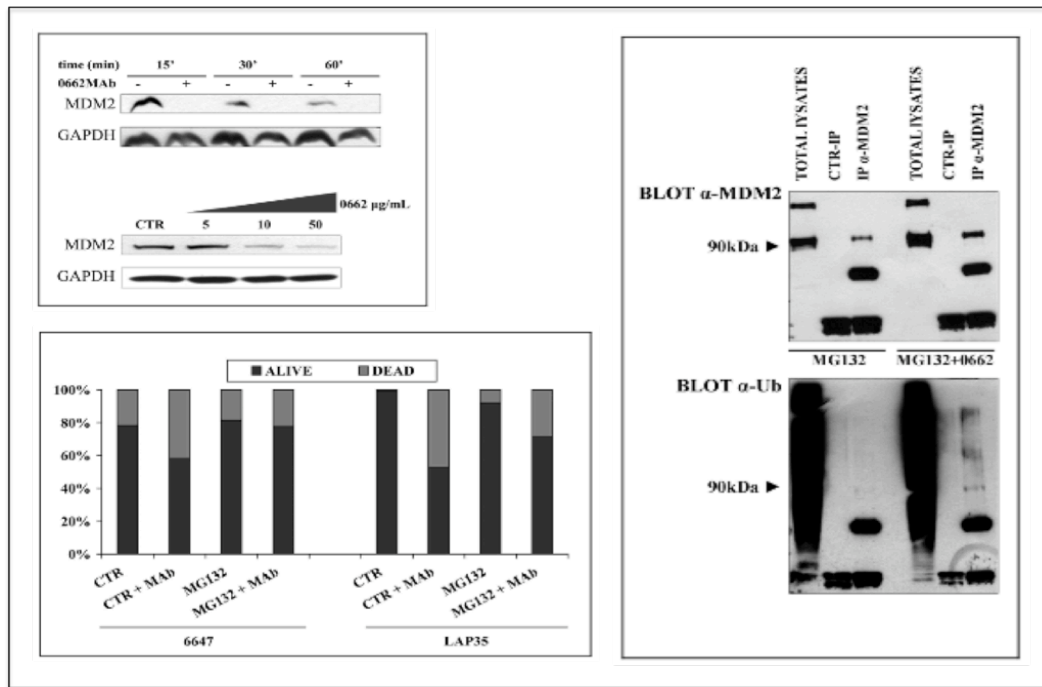


Figure 12. MDM2 expression in ES cell lines. Upper-left panel: whole cell lysates from untreated (-) or MAb treated (+) LAP35 cells and whole cell lysates from 6647 cells, untreated or treated with increasing concentration of 0662 MAb; right panel: Western blot evaluation of MDM2 (upper panel) and ubiquitin (lower panel) on total cell lysates, anti-MDM2 or anti-IgG immunoprecipitates from LAP35 cells treated with MG132 alone or plus 0662 MAb. Lower-left panel: Histogram depicting 6647 (left) and LAP35 (right) percentage of viable cells (vital cell counting) before and after a 16 h treatment with 10 µg/mL 0662 MAb, alone or in combination with MG132.

Besides p53, many studies report that MDM2 serves as a ubiquitin ligase also for the IGF-1R(109-111), thereby causing its degradation by the proteasome. On these bases, the present PhD project aims to:

- Evaluate IGF-1R modulations in response to 0662 mAb treatments in ES cells;
- Identify IGF-1R effectors positively or negatively regulated, and figure out what is the significance of this modulation;
- Dissect the mechanism by means of which CD99 starts its signalling and assess its fate when triggered by mAbs ;
- Investigate the effects of anti-CD99 mAb treatments in normal cells, in order to rule out possible concerns about toxicity related to the employment of these antibodies.

MATERIALS & METHODS

Cell lines and primary cell cultures.

SK-ES-1, SK-N-MC and RD-ES were obtained from the American Type Culture Collection (Rockville, MD, USA). TC71 and 6647 ES cell lines were a generous gift from T.J. Triche (Children Hospital, Los Angeles, CA, USA); Peripheral neuroectodermal tumor cell line LAP-35 was previously established and characterized at the Istituti Ortopedici Rizzoli, Bologna, Italy. The 6647 variant 6647/CD99^{low}, was previously obtained in our laboratory after a long and continuous exposure to 0662 mAb as previously described (40). The stably expressing CD99 U2/CD99wt57 was previously established in our laboratory (35). Murine C3H10T1/2 cells transfected with EWS/FLI-1(C3H10T1/2 EF) were provided by F. Lecanda (University of Navarra, Pamplona, Spain). ES cell lines have been tested for mycoplasma contamination (Mycoplasma detection Set, Takara Bio Inc.) and have been authenticated by STR PCR analysis. Cells were cultured in IMDM (Gibco), supplemented with 100 units/ml penicillin, 100 µg/ml streptomycin and 10% inactivated fetal bovine serum (FBS) (Lonza). Bone marrow-derived human mesenchymal stem cells were obtained from healthy donors or patients with benign bone lesions. After washings, cells were plated in α -MEM (Gibco), supplemented with 100 units/ml penicillin, 100 µg/ml streptomycin and 20% inactivated fetal bovine serum (FBS) (Lonza). Primary hMSC cell cultures were characterized for mesenchymal markers as well as for their differentiative ability and used within 6 *in vitro* passages.

Lentiviral infections, transient and stable transfections

All stable transfections were performed using Calcium Phosphate transfection Kit (*Invitrogen*): LAP35 cells were transfected with pCMV or pCMV-MDM2 and maintained in selective medium containing neomycin [250 µg/ml]; 6647 was transfected with pBABEpuro-HRasN17, and cells expressing the mutant form of Ras were selected with puromycin [500 ng/ml]; U2/CD99 wt57 were derived from the osteosarcoma cell line U2-OS transfected with pcDNA3-CD99 and maintained in selective medium containing neomycin [500 µg/ml]; C3H10T1/2 EF cells were transfected with pcDNA3-CD99 and cultured in medium containing neomycin [500 µg/ml]; 6647 cells were transiently transfected with pcDNA3/His-Ub by using Lipofectamine 2000 (*Invitrogen*), 48 hours later treatments and nichel-beads pull down were performed; pLKO.1 shAtg7-E8 (TET-ON inducible) and pGIPZ sh SCR (constitutive) were transfected on HEK293T cells to generate lentiviral supernatant to infect ES cell lines. Genetically-modified cells were employed for 0662-mAb treatment and subsequent apoptosis assays, cell count or western blot analysis.

0662 mAb treatments

The anti-CD99 0662 monoclonal antibody (mAb) was produced in the Unite' INSERM 343, Hospital de l'Archet, Nice, France, and cauterized during the Human Leukocyte Differentiation Agents International Workshop in 1989 and 1993 (*Gelin C et al., 1995*). Treatments with 0662 mAb were either performed on adherent cells or in suspension. Particularly, cells were washed in PBS, and detached from substrate with trypsin-EDTA 0.5%, counted and seeded at final concentration of 5×10^6 /mL and incubated in IMDM 10% FBS with or w/o 0662 mAb. After the indicated time-points, control and treated samples were washed in PBS and employed for Annexin-V/propidium iodide (PI) evaluation (Mebcyto apoptosis Kit, MBL) by flow cytometry, trypan blue cell count, cell viability analysis (MTT assay kit, Roche) or for protein/RNA extraction. To evaluate the proteasome- and lysosome-mediated degradation, treatments have been performed with 0662 alone or together with

MG132 [20 μ M] and lysosome inhibitor [100 μ M], both alone or combined; lysosome inhibitor was composed by leupeptin and pepstatin. Unless differently specified, all treatments have been carried out with 0662 [3 μ g/ml]. Morphological alterations were analyzed by electron microscopy. LC3-II positive autophagosomes were detected by immunogold staining on ultrathin section by electron microscopy.

Electron microscopy analysis.

6647 or LAP35 cells treated with 10 μ g/mL of 0662 mAb for 30 min were fixed with 2.5 % glutaraldehyde in 0.1 M cacodilate buffer, pH 7.4, postfixed with 1% OsO₄, dehydrated to absolute ethanol and embedded in Epon. For immunogold labeling LAP35 cells untreated or exposed to anti-CD99 0662 mAb (10 μ g/mL) for 3h were fixed with 4 % paraformaldehyde and immunolabeled with anti-LC3B primary antibody; a goat anti-rabbit IgG conjugated with 5 nm colloidal gold particles was used as secondary antibody (GE Healthcare Biosciences, USA). Signal was amplified with Silver Enhancer kit (GE healthcare Biosciences). After immunolabeling cell monolayers were fixed with 1 % glutaraldehyde in 0.1 M Na-phosphate buffer, postfixed with 0.5% OsO₄, dehydrated to absolute ethanol and embedded in Epon. Ultrathin sections were stained with uranyl acetate and lead citrate before electron microscopy observation with a Zeiss EM109 electron microscope.

Immunofluorescence staining.

Cells were seeded on poly-D-lysine-coated coverslips (BD Biosciences) and after 24h stimulated with anti-CD99 mAb. The stained preparations were observed with a confocal microscopy Nikon A1R and/or with a fluorescence microscopy Nikon Eclipse 90i or 300 (Nikon); the fluorescence was visualized with a digital imaging system using an inverted epifluorescence microscope (Nikon Eclipse 300) with 63X/1.4 oil objective (Nikon Eclipse Ti-U, Nikon, Japan) and Omega Filter pinkel Set XF66-1 triband (Omega Optical Inc., Brattleboro,VT, USA). Images were captured with a back-illuminated Photometrics Cascade CCD camera system (Roper

Scientific, Tucson, AZ, USA) with 500ms of exposure time and elaborated with Metamorph acquisition/analysis software (Universal Imaging Corp., Downingtown, PA, USA). After washing in PBS, cells were fixed in 4% paraformaldehyde and permeabilized in TritonX-100 0.15%-PBS, blocked in 4% BSA and incubated with specific antibodies for immunofluorescence analysis: anti-CD99 primary antibody (Abcam, clone 12E7) + anti-mouse PE; anti-Lamp-1 polyclonal antibody (Santa Cruz Biotechnologies) + anti-rabbit FITC (Dako); anti-Lamp-1PE (BD Pharmingen); anti-Rab4 polyclonal antibody (Thermo Scientific) + anti-rabbit FITC(Dako); anti-Rab11 (Abcam) + anti-rabbit FITC(Dako); anti-clathrin polyclonal antibody (Cell Signaling) + anti-rabbit FITC(Dako); anti-caveolin-1 (BD-transduction labs) + anti-rabbit FITC(Dako); anti-IGF-1R (Santa Cruz Biotechnologies, clone C20) + anti-rabbit FITC(Dako); anti-IGF1RPE (Pharmingen); anti-Rab5 (Thermo Scientific) + goat anti-rabbit Dy Light 350 (Thermo scientific). Nuclei were counterstained with Hoechst 33342.

Western blotting and immunoprecipitation.

Cells were lysed with Phospho-protein extraction Buffer (Upstate) supplemented with protease-phosphatase cocktail inhibitor (Sigma). Proteins of interest were detected with specific antibodies: anti-p53 (DO-1) monoclonal antibody (SEROTEC), anti-ser15-P p53 polyclonal antibody (Cell signaling Technologies), anti-p21 (H-164) polyclonal antibody (Santa Cruz Biotechnology), anti-Ub (P4D1) monoclonal antibody (Santa Cruz Biotechnology), anti-mdm2 (OP-46) monoclonal antibody (Calbiochem) and anti-gapdh (FL-335) polyclonal antibody (Santa Cruz Biotechnology), anti-pan RAS (Ab-1) monoclonal antibody (Oncogene), anti-Fli1 (C-19) rabbit polyclonal antibody (Santa Cruz Biotechnology), anti-ATG7 (2631) polyclonal antibody (Cell signaling Technologies), anti IGF-1R (C-20) polyclonal antibody (Santa Cruz Biotechnology), anti - ERK (Cell signaling), anti - thr202-tyr204-pERK (Covance). For immunoprecipitation, 500 μ g or 900 μ g of cell lysates were incubated for 16 hours with Protein G-Plus agarose beads (Calbiochem) in the

presence of 2 µg anti-CD99 (abcam) or 3 µg anti-IGF-1R antibody (Calbiochem). Immunoprecipitates and 40 µg total lysates were then resolved on a 10% Tris-HCl gel and immunoblotted with specific antibodies.

ELISA assay.

To determine the CD99 internalization, ELISA assays were performed in 6647 cell line: 70000 cells/time-point treatment were seeded in multi 24 plates and mAb treated after 24h for the indicated times; cells were then starved for 3 hours and washed in TBS 1X, subsequently they were fixed in 3.7% TBS-paraformaldehyde and blocked in 1% TBS-BSA. After the incubation with the anti-mouse alkaline phosphatase-conjugated secondary antibody, the relative substrate (BIO-RAD Cat# 172-1063) was added to the cells. The reaction was stopped by adding NaOH 0.4 N, then absorbance was read at 405 nm.

Nichel-beads pull down.

Co-treatments with 0662 [3 µg/ml] and MG132 [20 µM] + lysosome inhibitor [100 µM] have been performed in 6647 cell lines, then cells were lysed in Buffer A (HNTG+MG132/leu/pep + "complete" cocktail phosphatase inhibitors (Sigma) +PMSF+Na₃VO₄); in parallel, nichel beads (Qiagen) have been washed 3 times in PBS and one time in Buffer A, then resuspended in Buffer A and added to each lysate previously solubilized in Buffer A (500 µg). After an over-night rotate incubation at 4°C samples have been washed 3 times in Buffer B (HNTG+Inhibitors+Imidazole 20 mM pH 8), then Buffer C (HNTG+Inhibitors+Imidazole 250 mM) was added to the pellets; the suspensions have been vortexed and spinned, then resuspended in Buffer C + laemli buffer, boiled and resolved on a 10% Tris-HCl gel.

Flow cytometry analysis.

The expression of CD99 was analyzed by indirect immunofluorescence and flow cytometry analysis (*FACS Calibur, Becton Dickinson*): cells were counted and a

pellet of 500000 cells was obtained; then, they have been resuspended using the anti-CD99 O13 monoclonal antibody (mAb) (Covance), 1: 80 + Goat anti-Mouse IgG (H+L) FITC (diluizione 1:100) (*Thermo Fisher Scientific Inc*). Both incubations were stopped by adding serum-free medium and, as a final step, cells have been resuspended in PBS-diluted ethidium bromide [1µg/ml], before proceeding to FACS analysis.

RNA extraction and Real Time PCR.

RNAs were extracted using TRIZOL reagent (Life Technologies, cat# 15596018). Pre-designed TaqMan probes were chosen for IGF-1R (Taqman assay # Hs00181385_m1) and for GAPDH endogenous control (Taqman assay # Hs99999905_m1) (Applied Biosystems). Samples were analyzed using an ABI Prism 7900 Sequence Detection System (Applied Biosystems, Foster City, CA), according to manufacturer's instructions. Expression levels of target genes were normalized to that of glyceraldehyde 3-phosphate dehydrogenase (GAPDH), and the relative quantification analysis was performed on the basis of the $\Delta\Delta CT$ method. cDNA from untreated cells was used as calibrator for the comparative analysis.

Plasmids

pLKO.1 shAtg7-E8 (TET-ON inducible) and pGIPZ sh SCR (constitutive) were kindly provided by Bruno Calabretta, Philadelphia, USA; pCMV or pCMV-MDM2 were kindly provided by Dr Fabiola Moretti, Rome; pBABE-HRasN17 was kindly provided by Dr Kurosaki, Moriguchi, Japan; pcDNA3/His-Ub was kindly provided by Dr Andrea Morrione, Philadelphia, PA.

Statistics

Differences among means were analyzed using 2-tailed Student's *t* test. Fisher's exact test was used for frequency data. A *P* value less than 0.05 was considered significant.

RESULTS

1. IGF-1R/MDM2 relationship in ES

In order to confirm the well documented role of MDM2 as a negative regulator of IGF-1R also in the ES cellular context, we took advantage of a Ewing cell line stably expressing WT-MDM2 (LAP35-MDM2) or carrying the pCMV empty vector (LAP35-E.V.) to evaluate IGF-1R protein expression. As shown by the western blot analysis in Figure 13, LAP35 cells overexpressing MDM2 not only present a marked p53 downregulation, but they are characterized also by decreased levels of IGF-1R expression.

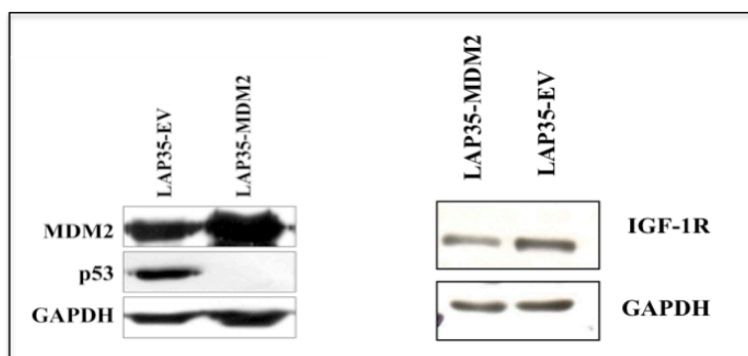


Figure 13. MDM2 downregulates IGF-1R in ES.

2. IGF1R modulations following 0662 mAb treatments

Once highlighted the inverse correlation between the ubiquitin ligase and IGF1R, and since preliminary data demonstrated the MDM2 downregulation in response to 0662 mAb treatments, we proceeded to evaluate IGF-1R modulations following CD99 triggering by 0662 mAb, both at mRNA and protein level. Real Time PCR and Western blot analyses performed, respectively, using cDNAs and lysates from LAP35 and 6647 cell lines previously treated with 0662 mAb for different times,

revealed a marked induction of the receptor at every time point of the treatment (Figure 14).

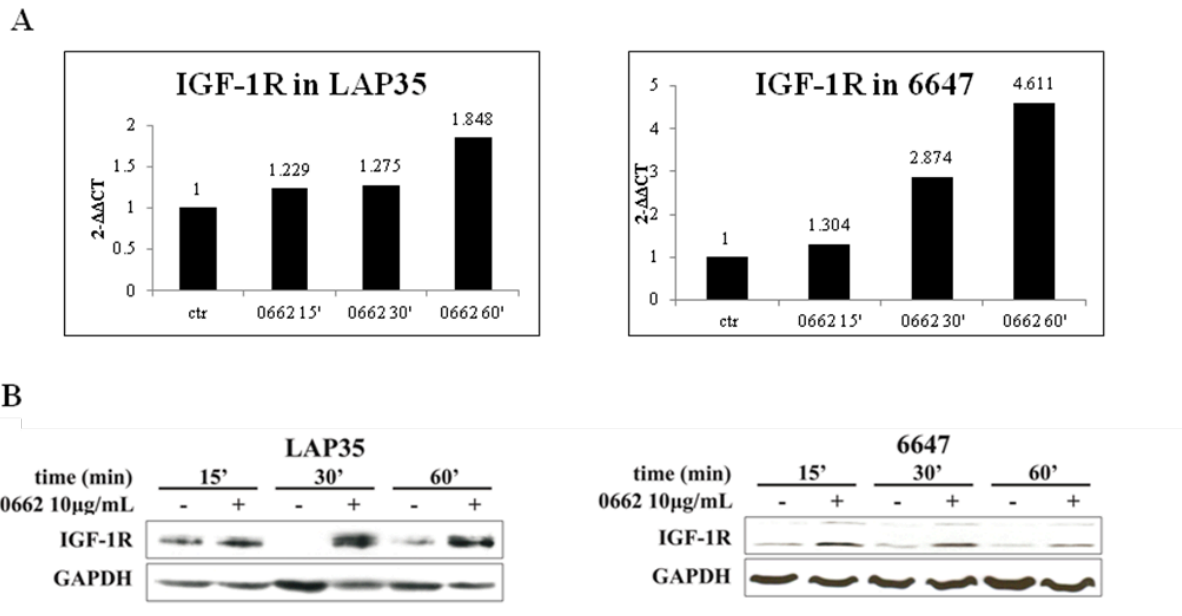
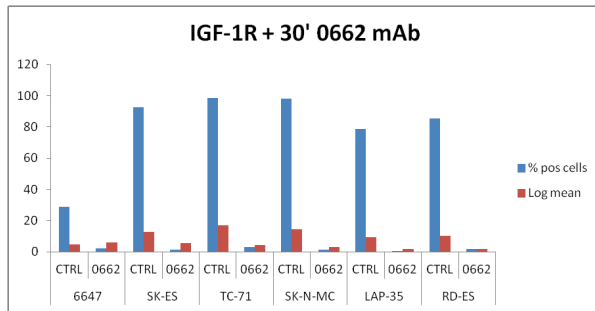
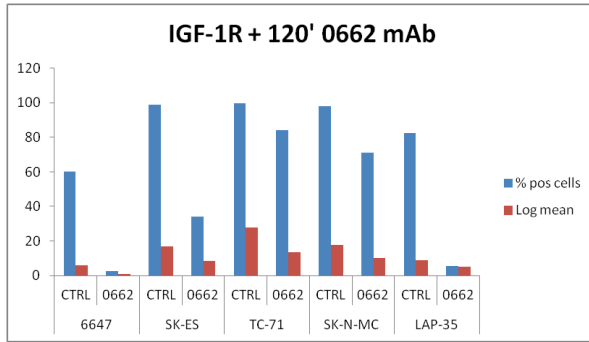


Figure 14. IGF-1R induction following CD99 engagement by 0662 mAb in 6647 and LAP-35. Upper panels: Graphs showing results of Real Time PCR; lower panels: western blot analysis confirming RT PCR data. All treatments have been carried out for 15-30-60 minutes with 0662 10 μ g/ml.

Concomitantly, flow cytometry analysis of IGF-1R carried out on a panel of 0662 mAb-treated ES cells resulted in a decrease of the receptor expression on the cell surface if compared to the respective untreated control; same phenomenon has been observed in a ES cell line obtained by continuous and long exposure to the 0662 mAb, 6647^{CD99^{low}}: despite the IGF-1R induction, together with ERK phosphorylation and MDM2 downregulation detected by western blot, the expression level of the receptor on the plasma membrane was significantly lower than that registered in 6647 (Figure 15).



		% pos cells	Log mean
6647	CTRL	28.94	4.86
	0662	2.28	5.92
SK-ES	CTRL	92.75	12.72
	0662	1.46	5.68
TC-71	CTRL	98.53	16.95
	0662	2.81	4.46
SK-N-MC	CTRL	98	14.42
	0662	1.42	2.99
LAP-35	CTRL	78.49	9.4
	0662	0.63	1.53
RD-ES	CTRL	85.5	10.02
	0662	1.7	1.57



		% pos cells	Log mean
6647	CTRL	60.18	5.97
	0662	2.71	1
SK-ES	CTRL	98.95	16.99
	0662	34.23	8.46
TC-71	CTRL	99.57	27.77
	0662	84.13	13.38
SK-N-MC	CTRL	98.15	17.89
	0662	70.98	10.12
LAP-35	CTRL	82.24	9.08
	0662	5.47	5.08

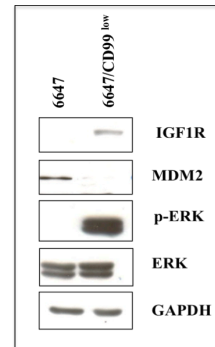
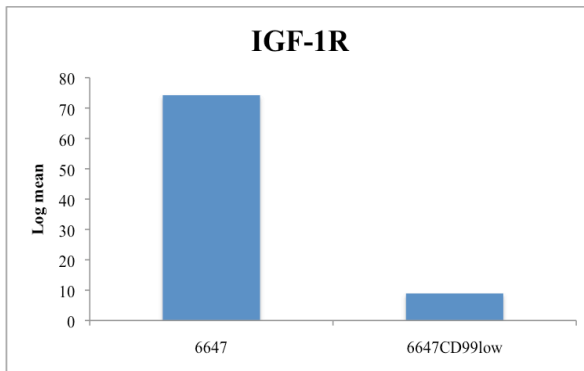


Figure 15. Flow cytometry analysis showing the IGF-1R decreased levels on the surface of ES cells. Western blot analysis of IGF-1R, p-ERK and MDM2 basal expression in 6647^{CD99low} are shown in the lower-right panel.

3. CD99 internalization after its recruitment by 0662 mAb

One of the issues not mentioned in literature and totally unknown was the CD99 fate following treatments; to get more insight, we explored the internalization hypothesis by using ELISA and immunofluorescence (IF) assays. Taking advantage of U2/CD99wt57, an osteosarcoma cell line derived from U2-OS and stably transfected with CD99 (Figure 16, left panel), we treated cells for 1h and 3h with 0662 mAb, then we proceeded to the receptor immunostaining: untreated U2/CD99wt57 showed

CD99 widespread homogeneously throughout the entire cell surface; after 1 hour of treatment it began to form aggregates right beneath the plasma membrane, moving into the cytoplasm after 3 hours (Figure 16).

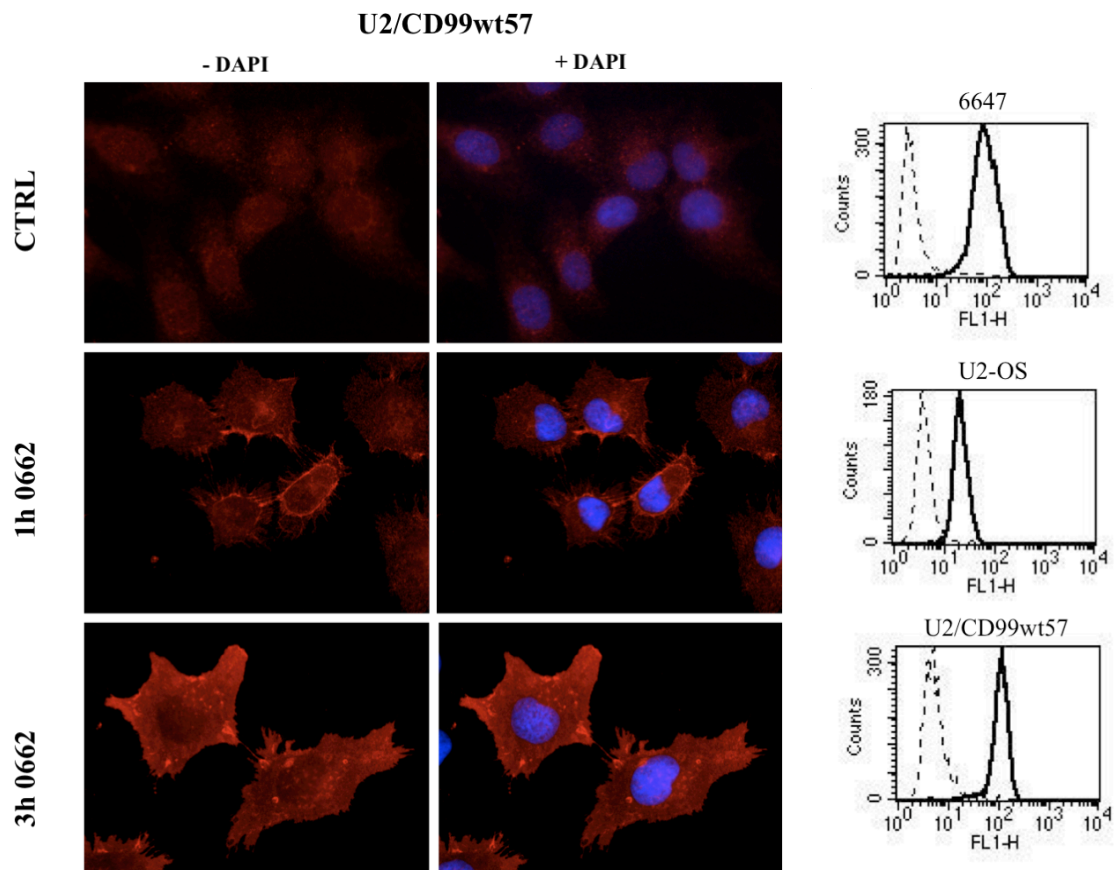


Figure 16. On the left, CD99 internalization in U2/CD99wt57 treated for 1h and 3h with 0662 3µg/ml. In the right panel FACS analysis of CD99 expression in 6647, U2-OS and U2/CD99wt57.

In parallel, in order to have a quantitative evaluation of CD99 internalization, we carried out some ELISA assays in 6647 mAb-treated, concluding that it internalizes into the cell in a time-dependent manner (Figure 17).

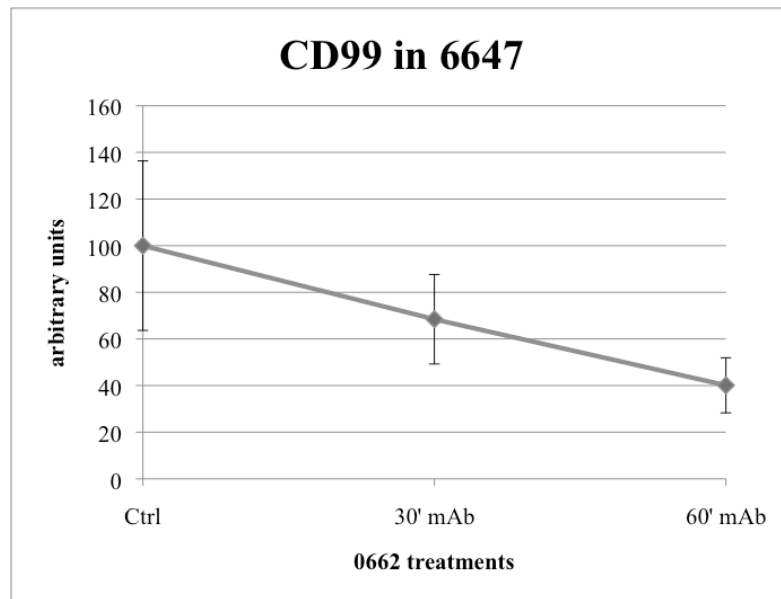


Figure 17. Time-dependent CD99 internalization in 6647 treated for 30' and 60' with 0662 3 μ g/ml.

4. CD99 stability

Once determined that CD99 translocates into the cytoplasm, it remained to be elucidated its stability. We set up a time-course treatment in 6647 and U2/CD99wt57 and, as depicted in Figure 18, we found out that CD99 protein levels decreased after 2 hours of treatment in 6647 and after 4 hours in U2/CD99wt57. The next step has been to figure out which mechanism could cause the observed CD99 reduction: to this purpose, we transiently transfected 6647 with a plasmid expressing a 6xHis-tagged ubiquitin (His-Ub), then I treated cells with 0662 mAb and proteasome/lysosome inhibitors at the same time and I subsequently performed a nickel beads pull-down to assess whether CD99 could be ubiquitinated as a consequence of the treatment. Anti-CD99 western blotting represented in Figure 18 confirmed that CD99 is poly-ubiquitinated, suggesting that its degradation could be proteasome-mediated.

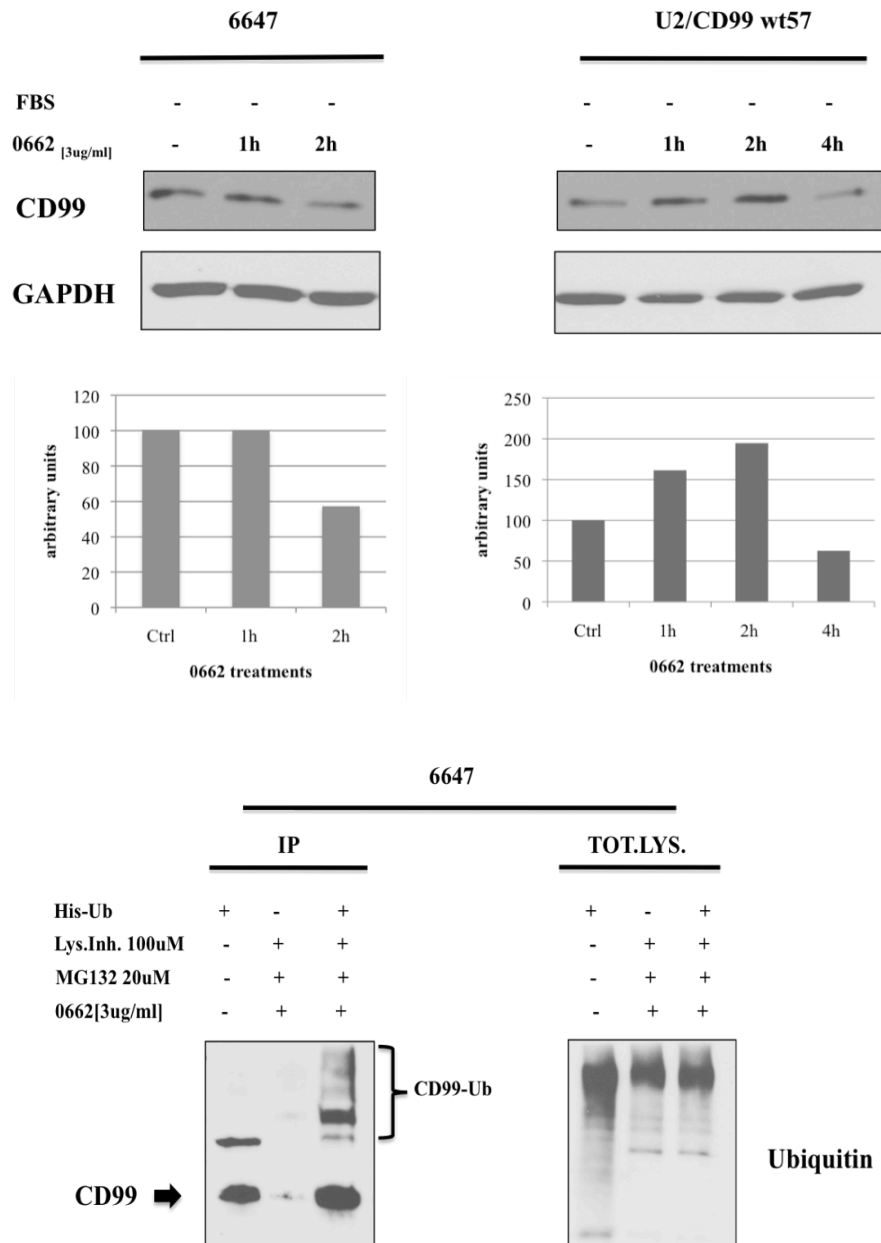


Figure 18. CD99 stability upon 0662 mAb treatments. (A) Western blots and respective densitometric analyses showing CD99 reduction in 6647 and U2/CD99wt57. (B) Nickel beads pull-down on lysates from 6647 transiently expressing a 6x His-tagged ubiquitin and treated with 0662 mAb and proteasome + lysosome inhibitors.

5. Role of lysosomes and endosomes in CD99 internalization process

In order to better define the mechanism by means of which CD99 protein amounts underwent the observed reduction, we explored, in parallel, two possible ways: the proteasome- and the lysosome-mediated degradation. 6647 have been treated with 0662 alone or in combination with MG132 (proteasome inhibitor), with lysosome inhibitor or both; based on the results shown in Figure 19, CD99 protein expression decreased following 2 hours of 0662 treatment alone, while the employment of the inhibitors visibly blocked the mAb-induced reduction of CD99. In particular, densitometric analysis emphasizes the CD99 rescue by the lysosome inhibitor, which seems to be predominant compared to that mediated by MG132.

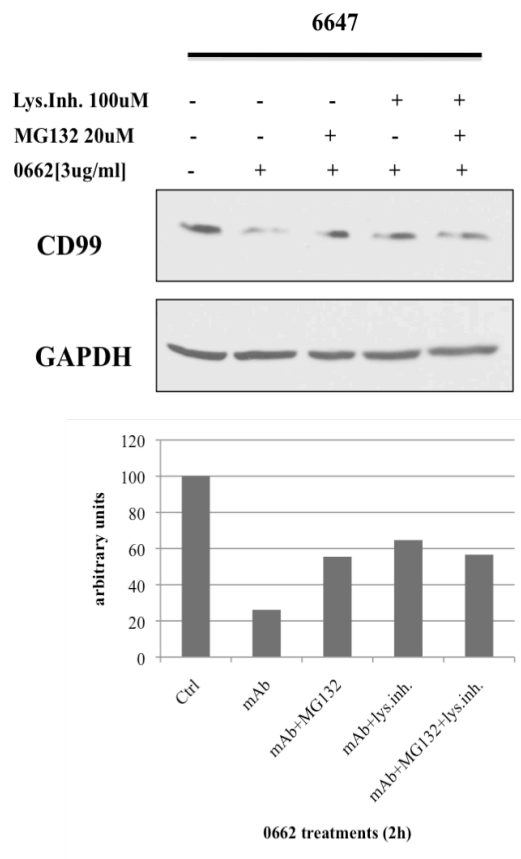


Figure 19. CD99 degradation is inhibited by blocking proteasome and lysosomes.

For this reason, I evaluated by confocal microscopy a colocalization between CD99 and Lamp-1, the latter considered the main marker of lysosomes, in U2/CD99wt57 0662-treated for 1 hour, 3 hours and 6 hours in presence of both MG132 and lysosome inhibitor. Normally the lysosome degradation is a very late event which becomes to be clearly visible after many hours upon a stimulus, in this case the two molecules colocalized after only 1 hour, increasing considerably their interaction in the other time points, concomitantly with the formation of enormous aggregates (Figura 20).

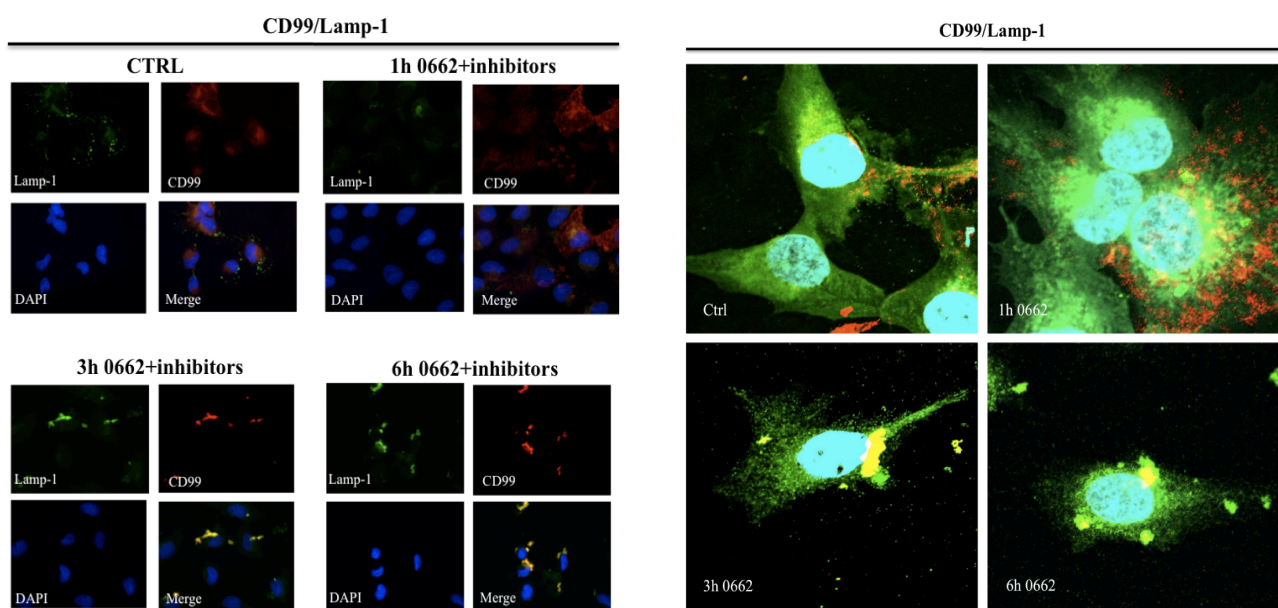


Figure 20. IF (left panel) and confocal microscopy (right panel) images of CD99/Lamp-1 colocalization upon 1h, 3h and 6h of 0662 treatment in combination with MG132 and lysosome inhibitor. The interaction is depicted as yellow dots, which become bigger in the last two time-points because of the employment of the inhibitors that favour the CD99 accumulation.

As a further confirm of its degradation, CD99 was not found to colocalize with Rab11, a late endosome marker implicated in recycling mechanisms, after 30 and 90 minutes of 0662 treatment. Notably, the internalization process resulted to be endosome-mediated, since CD99 was found associated to Rab4, an early endosome marker involved also in the biogenesis of endosomes, particularly after 30 minutes of

treatment (Figura 21).

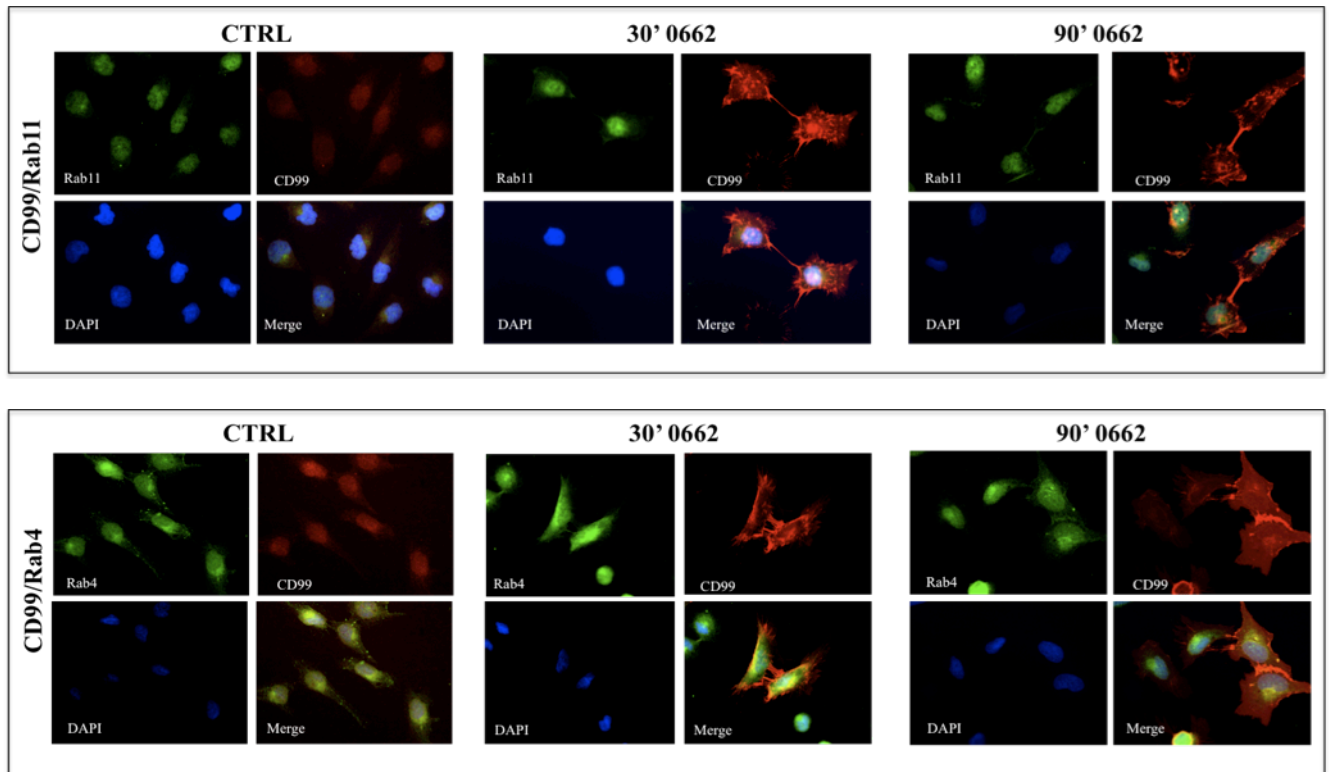


Figure 21. Evaluation of CD99/Rab11 (upper panel) and CD99/Rab4 (lower panel) colocalizations by IF assays upon 30 and 90 minutes of 0662 treatment. The interaction (yellow areas) is detected for CD99/Rab4, but not for CD99/Rab11.

6. CD99 internalizes both in a clathrin- and caveolin-1-dependent manner

After having demonstrated that CD99 undergoes an internalization process leading, as a final step, to its degradation by lysosomes, we examined the beginning of the entire process, in order to identify the endocytosis route mainly involved. The latter can occur through two different pathways: the clathrin-dependent and the clathrin-independent endocytic pathways; the first one requires the formation of clathrin-coated vesicles, while the second one takes place through the formation of the caveolae, invaginations of plasma membrane whose main component is caveolin-1.

We performed IF assays in U2/CD99wt57 0662-treated for 10, 30 and 60 minutes to test the eventual colocalization between CD99 and clathrin or caveolin-1, and, surprisingly, we found out that both pathways participated in the endocytosis process (Figura 22).

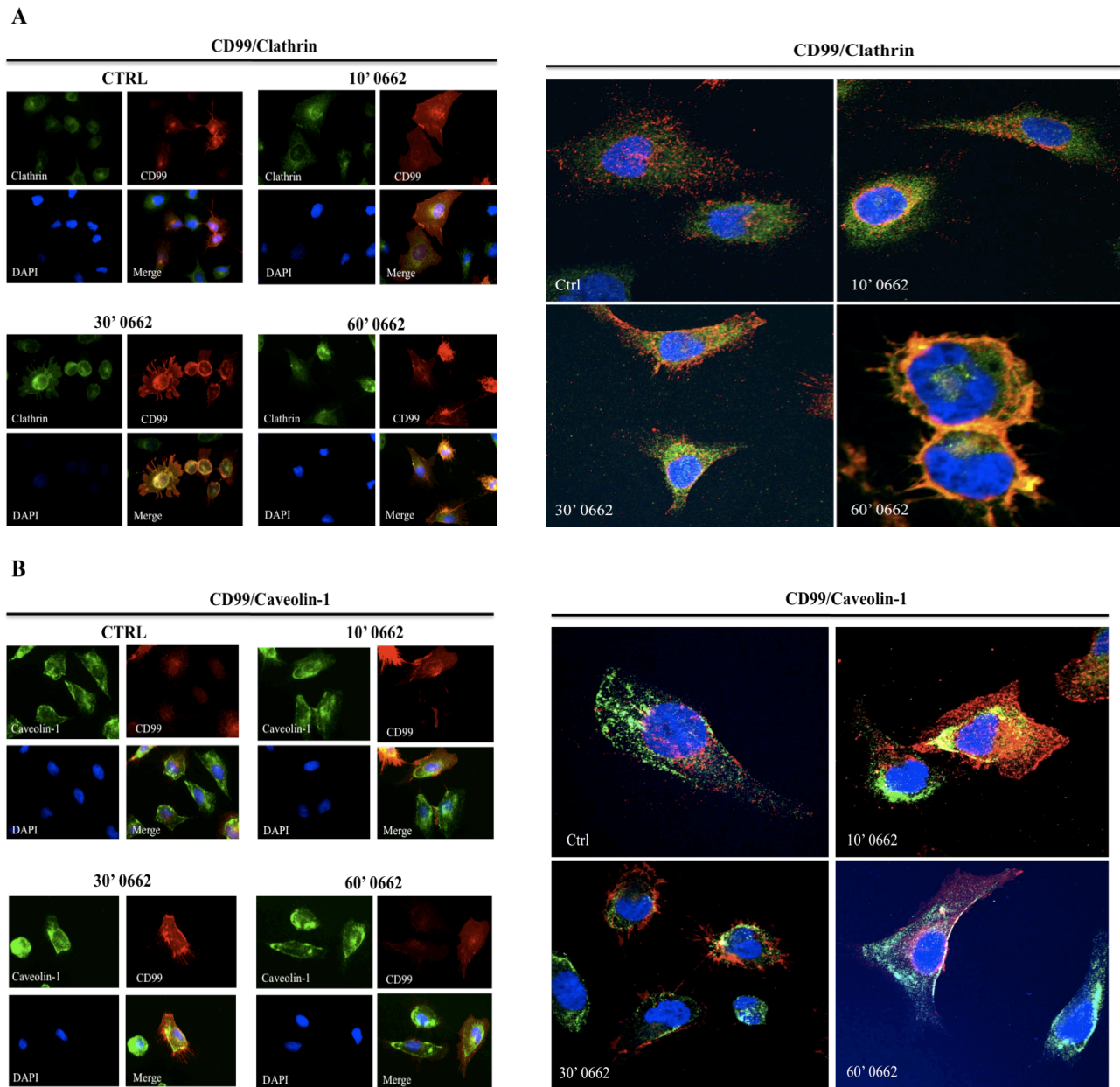


Figure 22. Evaluation of CD99/Clathrin (A) and CD99/Caveolin-1 (B) colocalizations upon 10, 30 and 60 minutes of 0662 treatment in U2/CD99wt57. On the right, confocal microscopy analyses confirm the results from IF assays depicted on the left.

7. CD99 and IGF-1R interaction upon 0662 treatment

Previously we reported an increase of IGF-1R in ES cell lines both at protein and mRNA level following treatments; notably, FACS analysis highlighted a decrease of its expression on the cell surface, suggesting that the receptor could possibly undergo an internalization process. Based on these results and considering the documented mAb-induced internalization of CD99, we explored the hypothesis of an interaction between the two receptors, which could likely share the same fate. Once again we carried out combined treatments using 0662 and MG132 + lysosome inhibitors for 1 hour, 3 hours and 6 hours and we evaluated the CD99/IGF-1R co-localization by IF assays in U2/CD99wt57: both receptors resulted homogeneously widespread throughout the cell surface in the untreated control cell line, while after 1 hour of treatment CD99 is visible in the form of aggregates beneath the cell surface, even if there is no trace of interaction with IGF-1R; on the contrary, the co-localization is evident into the cytoplasm after 3 hours of treatment, and it is still slightly present in the last time point (Figure 23).

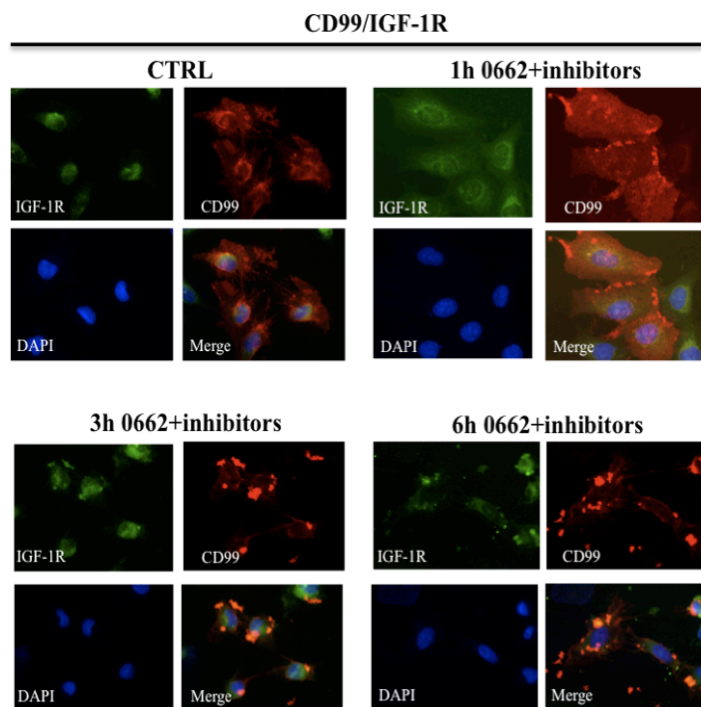


Figure 23. CD99/IGF-1R double staining upon 1, 3 and 6 hours of 0662 and MG132+lysosome inhibitor treatments.

To further confirm this result, we performed an immunoprecipitation (IP) anti-IGF-1R using lysates from 6647 previously treated with 0662 for 2 hours; anti-CD99 western blot analysis showed a marked interaction between the two molecules following treatment, corroborating the initial hypothesis (Figura 24).

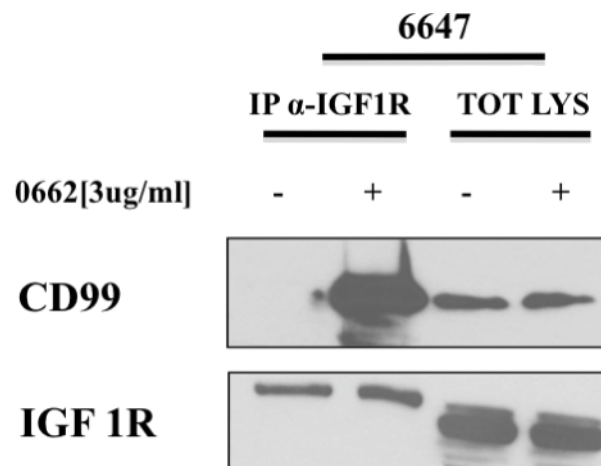


Figure 24. Western blotting α -CD99 showing the CD99/IGF-1R strong interaction after IP α -IGF-1R on lysates of 6647 previously treated for 2 hours with 0662 mAb.

8. IGF-1R is not degraded by 0662 mAb treatments

Once determined the IGF-1R internalization and its interaction with CD99 upon treatments, we then proceeded to investigate the observed process in details. In order to prove that the complex IGF-1R/CD99 could be internalized inside the endosomes, we performed a triple staining to detect the two receptors and Rab5, an early endosome marker involved in the biogenesis of endosomes. Confocal microscopy analysis on U2/CD99wt57 mAb-treated for 30, 60 and 90 minutes revealed that not only IGF-1R and CD99 formed a complex, confirming previous results, but each of them colocalized also with Rab5 (Figure 25).

CD99/IGF-1R/Rab5

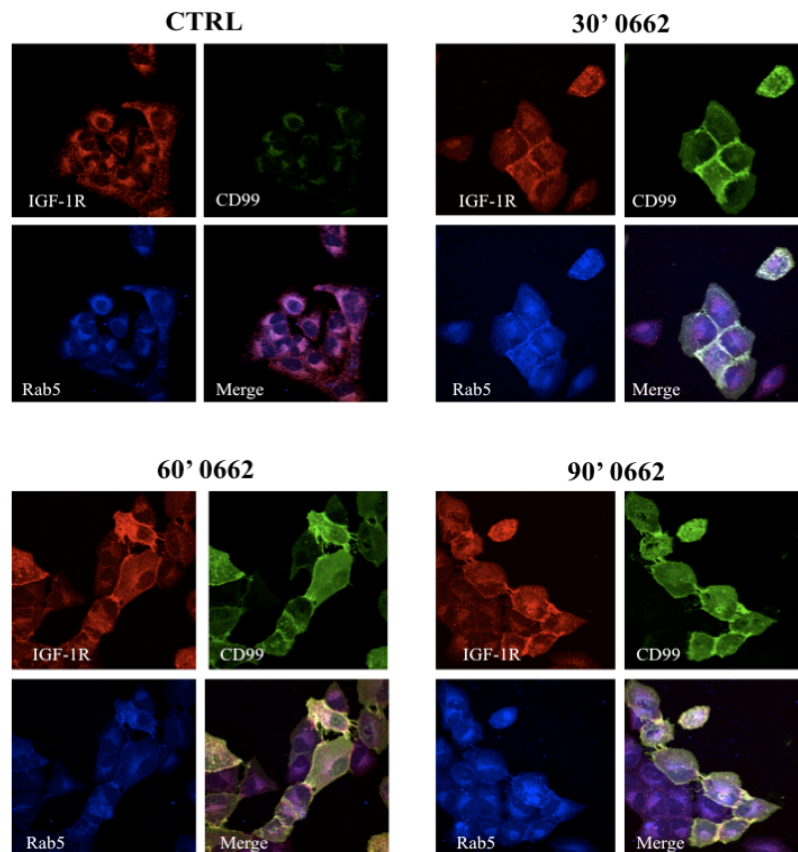


Figure 25. CD99/IGF-1R/Rab5 complex (merge) detected by confocal microscopy analysis in U2/CD99wt57 treated for 30, 60 and 90 minutes with 0662 [3 $\mu\text{g/ml}$].

The next step has been to evaluate whether IGF-1R could share the same fate of CD99 and undergo a lysosome-mediated degradation. We set up the same time-course treatment used to investigate the CD99/Lamp-1 co-localization in U2/CD99wt57, employing the combination of 0662 and MG132 + lysosome inhibitors, but in this case IGF-1R showed a different sorting, since none of the treatments caused the interaction with Lamp-1 observed for CD99 (Figure 26).

IGF-1R/Lamp-1

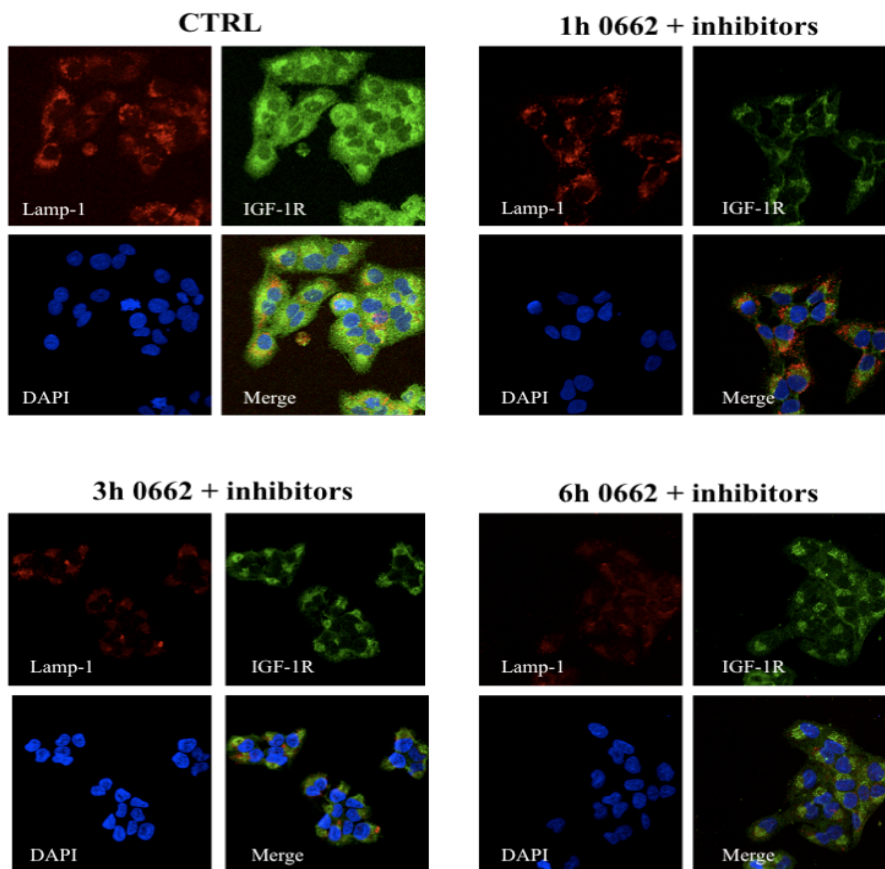


Figure 26. IGF-1R does not undergo lysosome-mediated degradation. Treatments were carried out with 0662 [3 $\mu\text{g/ml}$] and MG132 [100 μM] + lysosome inhibitor [20 μM] (leupeptin + pepstatin).

Conversely, confocal microscopy images depicted in Figure 27 show that IGF-1R is recycled on the cell surface, since it was found to colocalize with Rab 11, particularly after 60 and 90 minutes of treatment.

IGF-1R/Rab11

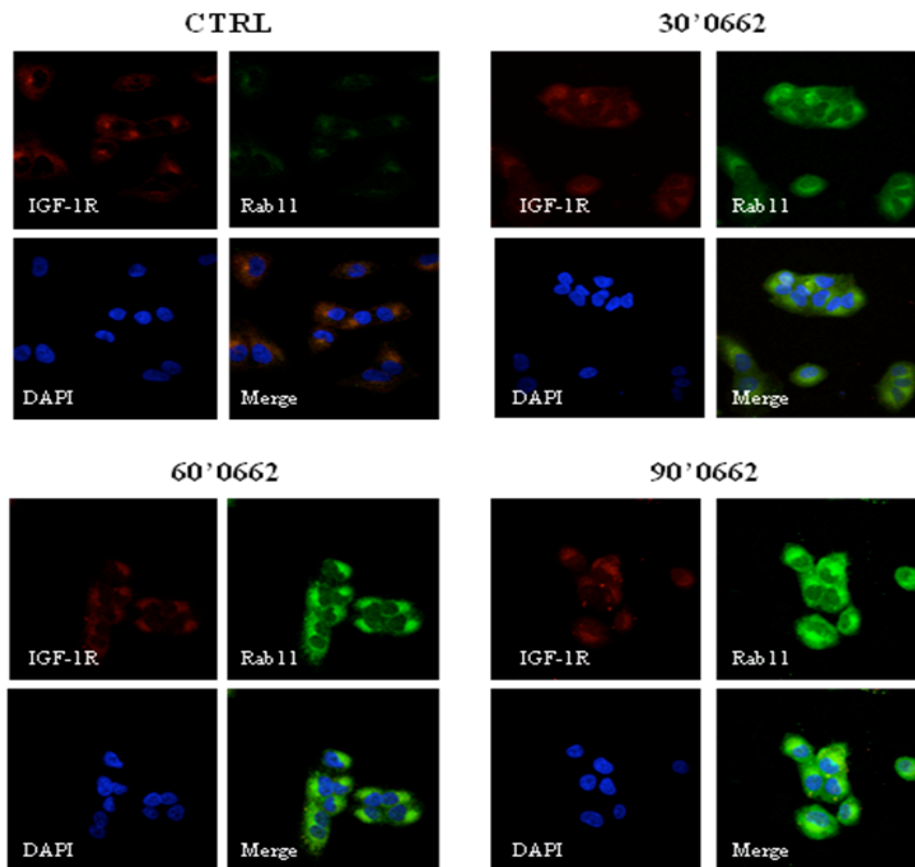


Figure 27. IGF-1R recycling on the cell surface.

9. Ras-MAPK signaling is activated in response to treatment

Considered the up-regulation of IGF-1R in protein and mRNA, and since it is not degraded following its internalization, but recycled on the surface, we investigated the modulation of Ras-MAPK pathway, one of the two main pathways associated to IGF-1R activation. As shown in Figure 25, 0662 mAb treatments in 6647 and LAP35 cell lines caused a strong Ras induction detected by western blotting and by IF assays, together with ERK phosphorylation and its translocation to the nucleus.

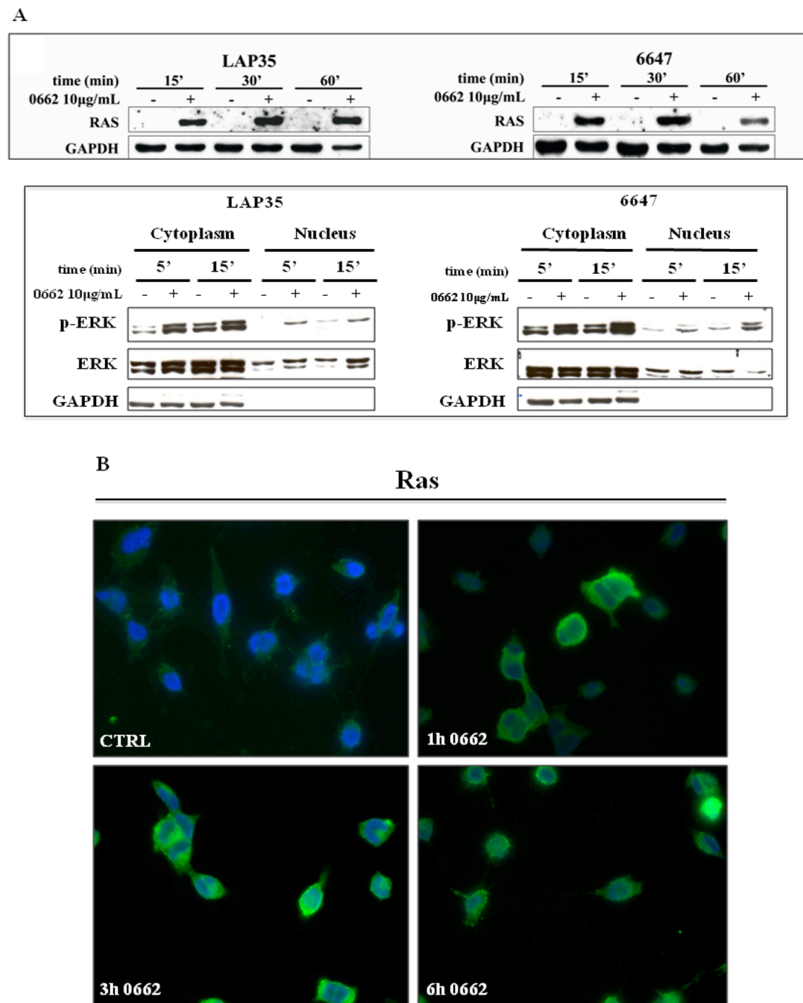


Figure 25. Ras-MAPK up-regulation in ES cells. (A) Western blotting depicting Ras and pERK induction following treatments; in the lower panel the cytosol/nucleus separation shows the ERK traslocation into the nucleus after its mAb-induced phosphorylation. (B) Ras activation detected in 6647 by IF assay.

A plethora of data in literature point out to a “non conventional” localization of Ras proteins; all Ras isoforms, infact, have been found to signal from a variety of intracellular membranes, including endosomes (112, 113). For this reason, we evaluated an eventual Ras interaction with CD99 upon or concomitantly with its induction by 0662 treatment. IF images in Figure 26 prove that the two molecules resulted physically linked in U2/CD99wt57 after 1, 3 and 6 hours of mAb exposure; this co-localization has been detected also by anti-Ras western blotting after anti-CD99 immunoprecipitation (IP), as a first instance, and anti-IGF-1R IP as a second

instance: both circumstances supported the supposed interaction (Figura 26).

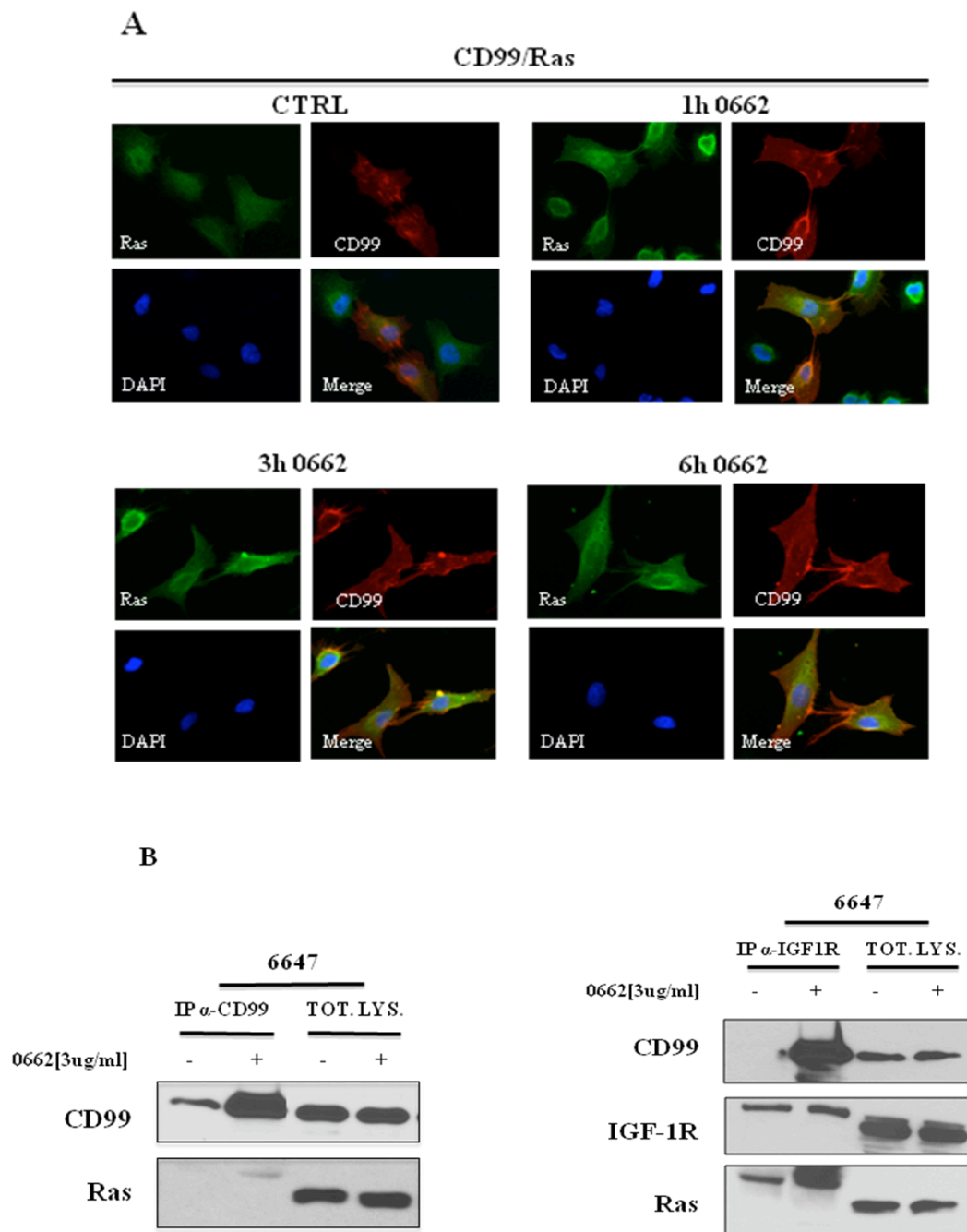


Figure 26. CD99/Ras interaction in ES and osteosarcoma cells.(A) IF images of 0662-treated U2/CD99wt57;(B) Anti-Ras western blotting after IP anti-CD99 (right) and IP anti-IGF-1R (left). In the first case the IP has been performed using 500 μ g of lysates, while in the second case 900 μ g have been used.

10. Cytoplasm vacuolization during 0662 mAb-induced cell death: autophagy hypothesis

Growing evidences demonstrate that the Ras prolonged and strong expression promotes cell death in many cellular contexts (93); particularly, Ras seems to be involved in autophagic cell death mechanisms (94, 95) and since 0662 mAb-induced cell death occurs in a caspase-independent manner, we tried to understand wheter the two events were functionally linked in the ES cellular context. Morphological analysis by electron microscopy showed an increase in cells with empty vacuoles, autophagosomes and less dense cytoplasm upon 0662-mAb treatment (Figure 27), but no features typical of apoptosis such as chromatin hyper-condensation, nuclei fragmentation, or cytoplasmic shrinkage.

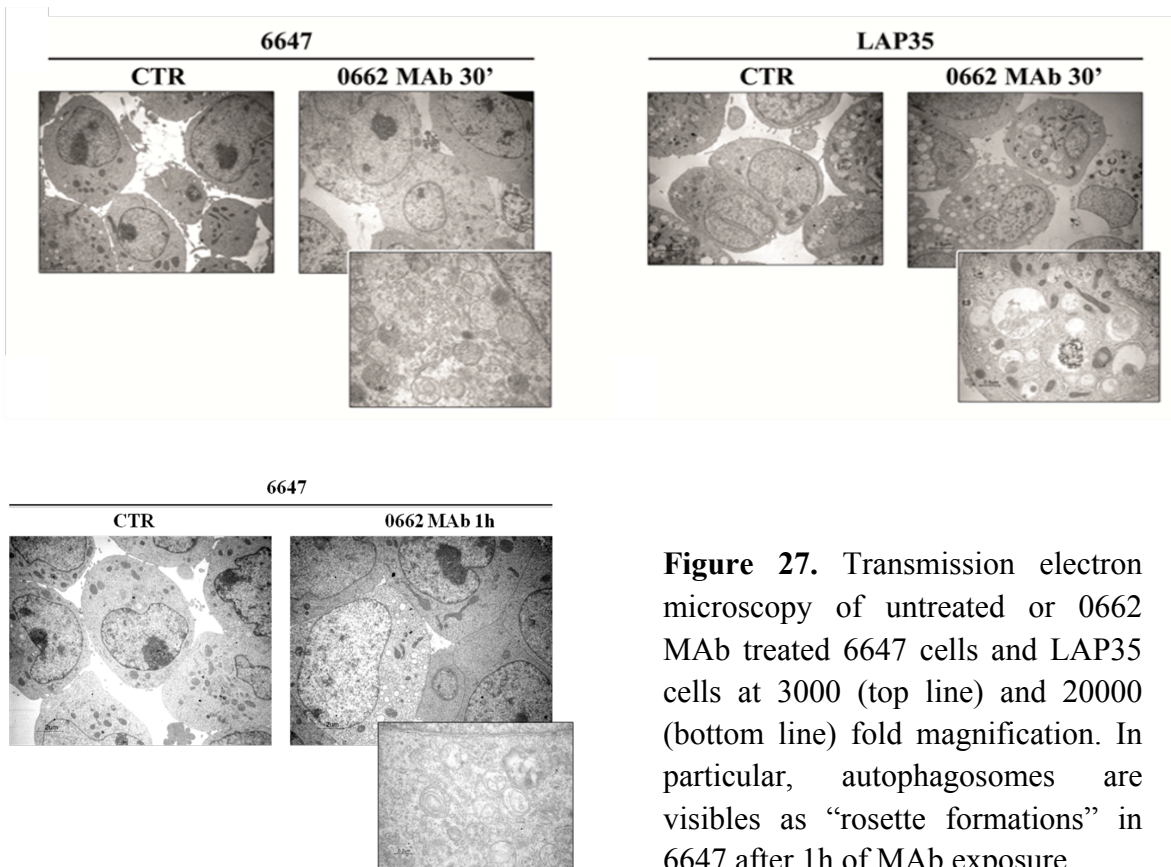


Figure 27. Transmission electron microscopy of untreated or 0662 MAb treated 6647 cells and LAP35 cells at 3000 (top line) and 20000 (bottom line) fold magnification. In particular, autophagosomes are visible as “rosette formations” in 6647 after 1h of MAb exposure.

Normally, upon induction of the autophagic process, LC3-IB is conjugated to the highly lipophilic phosphatidylethanolamine (PE) moiety of the autophagosome to generate LC3-II, which represents the main marker of autophagy; its analysis in ES cells treated with 0662-mAb revealed a punctate pattern of LC3-II distribution and its association with autophagic vacuoles (Figure 28), together with the accumulation in LAP35 cells (Figure 28).

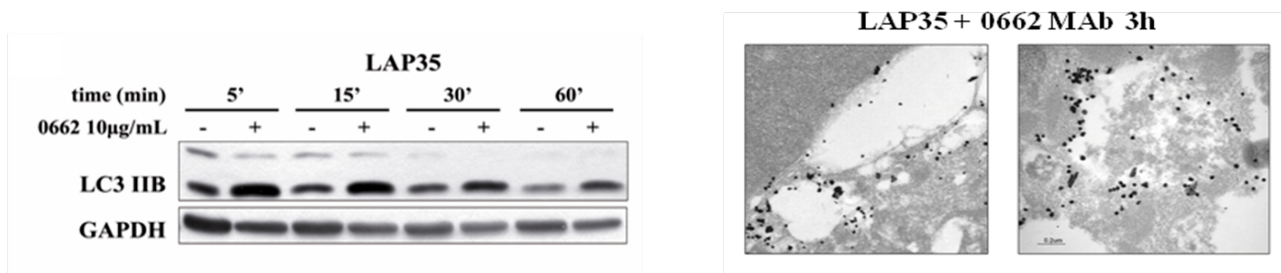


Figure 28. On the left: western blot analysis of LC3II on whole cell extracts from control (-) or treated (+) LAP35 is shown; Immunogold anti-LC3 staining of 0662 MAb-treated LAP35 cells at 20000 fold magnification is depicted on the right.

To validate all the evidence pointing to autophagy as the type of caspase-independent death caused by 0662 mAb employment, we stably silenced *Atg7*, an essential autophagy gene whose protein participates to the formation of LC3-II together with *Atg3* (E2-like conjugating activity) and *Atg12-Atg5-Atg16L* multimers (E3-like ligase activity)(114). *Atg7*-silenced cells still underwent cell death following CD99 engagement (Figure 29).

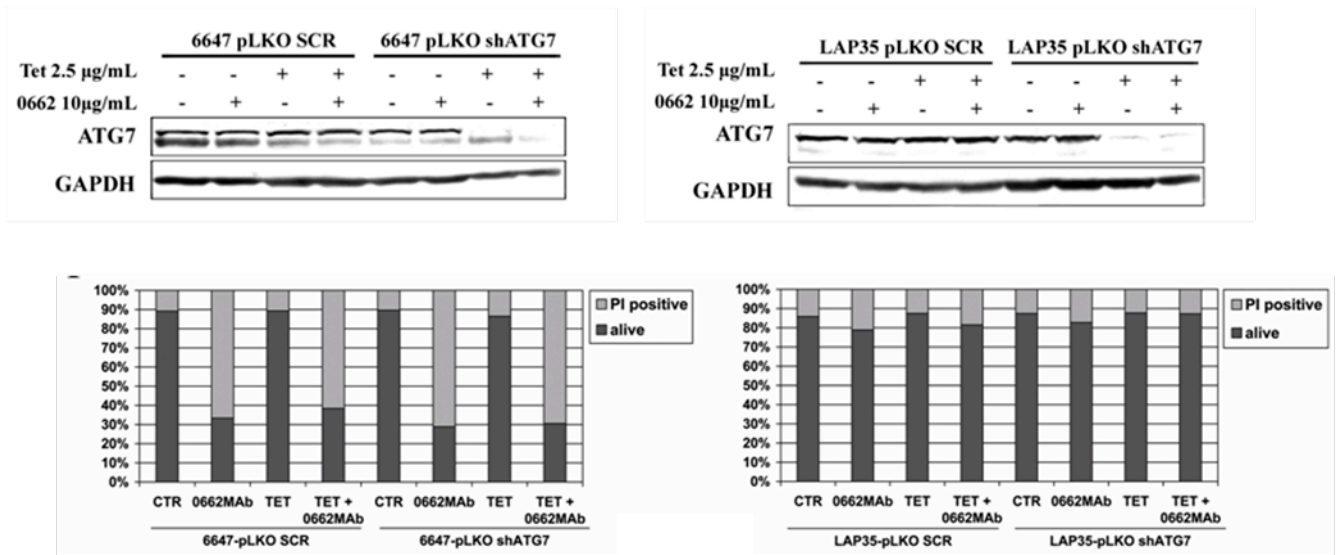
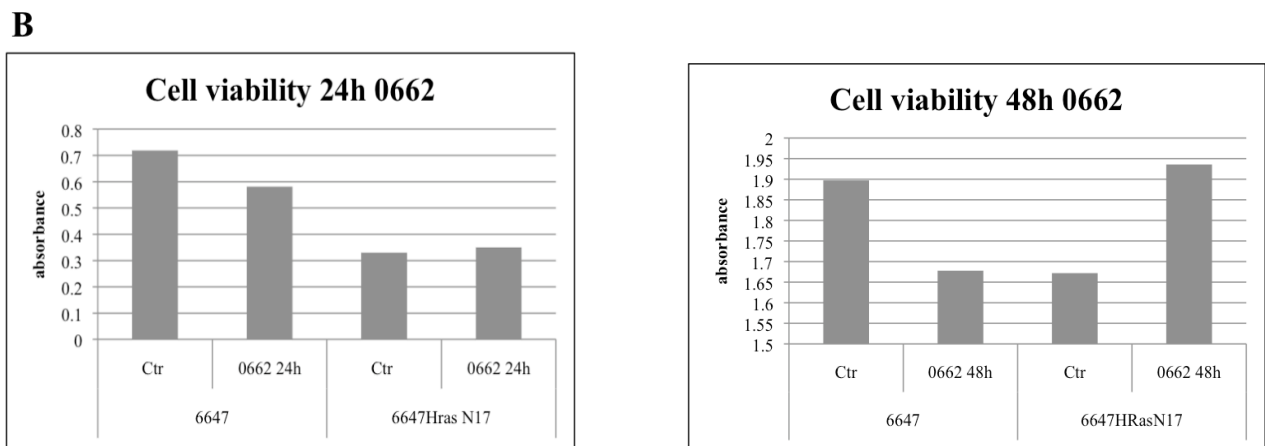
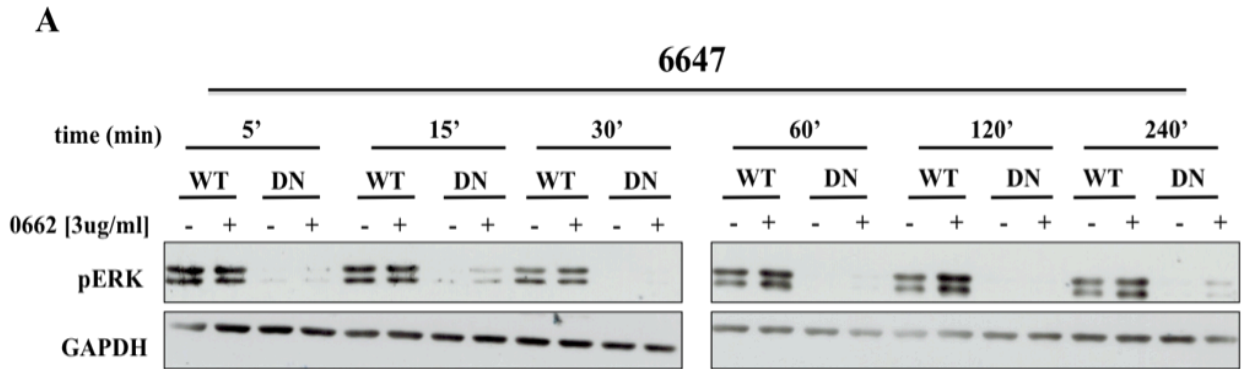


Figure 29. On the top, western blotting anti-ATG7 showing that the inducible silencing of *atg7* in 6647 and LAP35 cells was successful; on the bottom, cell death evaluation expressed as percentage of live (grey) or propidium iodide-positive (light grey) LAP35pLKO SCR, LAP35pLKOshATG7, 6647pLKO SCR, 6647pLKOshATG7 cells before and after treatment with 0662 mAb.

11. Ras has an active role in the observed cell death

The marked Ras induction and the observation that many vacuoles appeared devoid of cytoplasmic components suggested that CD99-mediated cell death might occur through hyperstimulation of macropynocytosis, as mentioned in literature for other cellular contexts (71). In order to confirm the role of Ras in the observed death we established a ES cell line (6647) stably expressing a Ras dominant negative construct, HRasN17. This mutant form of Ras, obtained by a substitution of serine 17 with asparagine, has a higher affinity for exchange factors than does wild-type Ras but it cannot interact with downstream effectors, resulting in the formation of unproductive complexes, thereby preventing the activation of endogenous Ras (115). HRasN17 construct expression in 6647 modified significantly cell viability upon 24 and 48 hours of 0662 mAb treatments, if compared to parental 6647 cell line, determining a reduction in the percentage of cell death (trypan blue positivity) after 24 hours of treatment (Figure 30).



C

6647		% Alive	% Dead
	Ctrl	98.3	1.7
	0662 24h	78.0	22.0

6647HRasN17		% Alive	% Dead
	Ctrl	89.5	10.5
	0662 24h	82.4	17.6

Figure 30. (A) Western blot analysis of p-ERK expression in lysates from 6647 and 6647HRasN17 mAb-treated/not treated demonstrating the reliability of the model. (B) MTT cell viability assay of 6647 and 6647/HRasN17 upon 24 and 48 hours of 0662 mAb exposure. (C) Trypan blue vital counts confirming the slight cell death rescue of 6647HRasN17: 20% of 6647 died after treatment, while the percentage of dead cells decreased to 7% for 6647HRasN17.

12. Mesenchymal stem cells are resistant to 0662 mAb-induced cell death

Since CD99 is broadly expressed at low levels also in normal tissues, to investigate the selectivity of therapeutic strategies based on CD99 targeting we evaluated the effect of 0662-mAb on human mesenchymal stem cells.

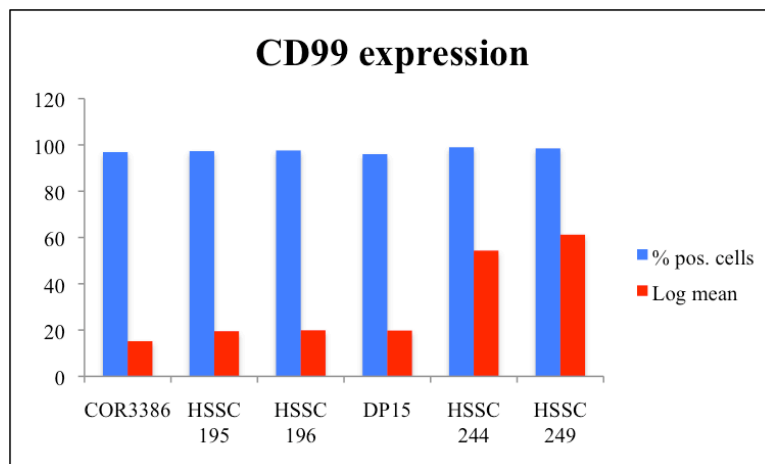


Figure 31. FACS analysis of CD99 expression detected in mesenchymal stem cells.

We took advantage of several human mesenchymal cell lines of distinct origins (CORION-3386, HSSC 195, HSSC 196, DP15, HSSC 244 AND HSSC 249) characterized by different levels of CD99 expression (Figure 31) and we tested them for annexin V/PI positivity following 0662 treatments, finding that not even those with a higher expression of the receptor (HSSC 244 and HSSC 249) were mAb-sensitive (Figure 32), since they did not displayed neither annexin V-PI staining nor activation of p-ser15-p53. On the contrary, CD99 triggering was still able to induce mild Ras activation and p21 induction (Figure 32).

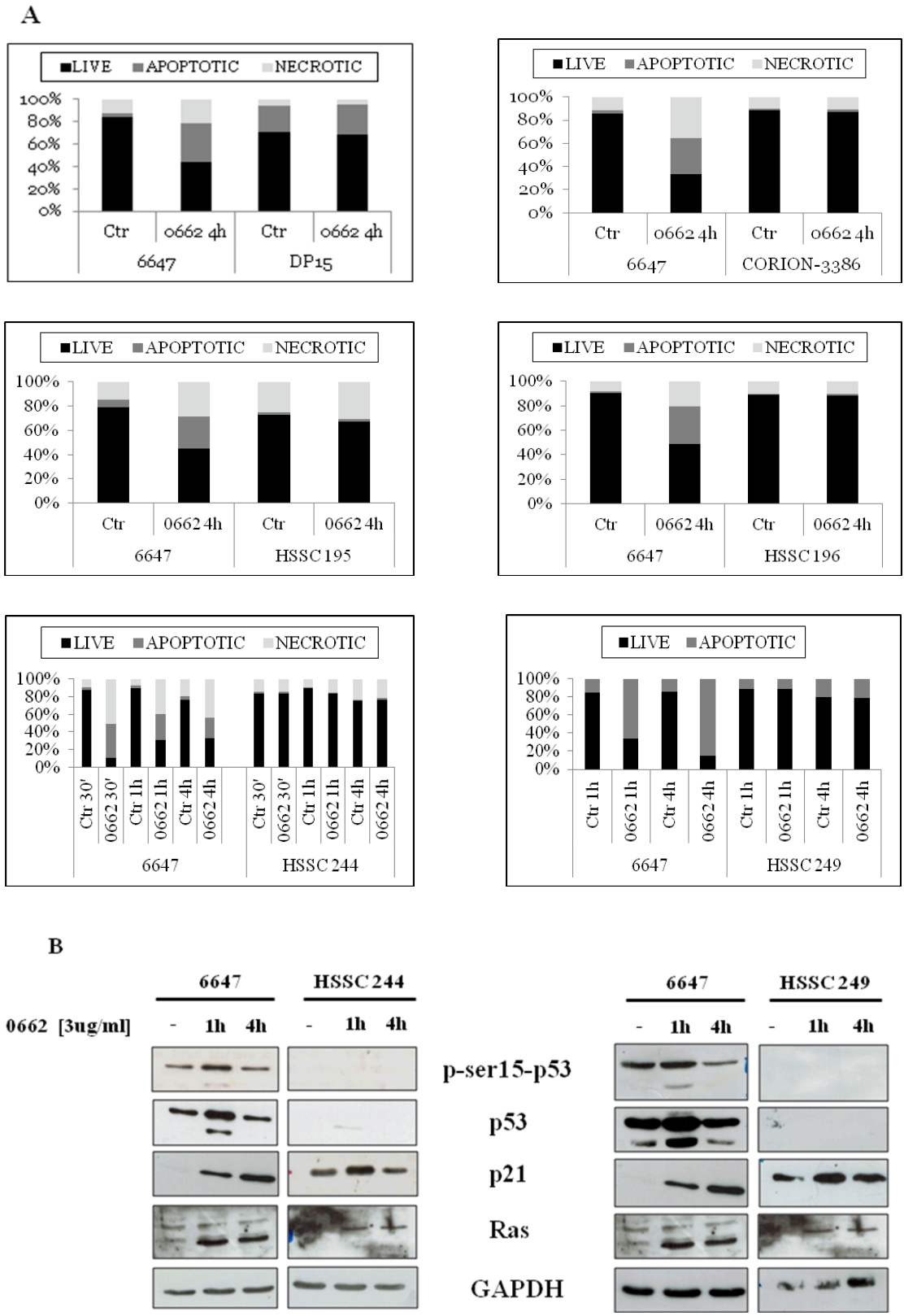


Figure 32. (A) Evaluation of Annexin V/PI positivity upon MAb 0662 treatment on 6647 and on hMSCs from different origins. (B) Western blotting analysis of Ras, p21, phospho-serine15-p53, and total p53 before (-) and after (+) treatment with 3µg/ml 0662 MAb on 6647 and two different hMSCs.

13. EWS/FLI1 favors the delivering of the CD99-induced cell death message

Based on the results obtained with human mesenchymal stem cells, we explored whether the CD99-induced cell death message requires an aberrant oncogenetic-driven cellular context. Considering the pivotal oncogenetic role of EWS/FLI1 in ES cells, we took advantage of a murine mesenchymal model, namely C3H10T1/2 EF CD99, transfected both with EWS/FLI1 and CD99 as reported in literature (40), demonstrating that treatment with 0662 mAb is sufficient to trigger cell death and to induce phosphorylation of serine 15 of p53 within 1 hour, together with a stronger Ras upregulation compared to that observed in HSSC 244 and HSSC 249 (Figure 33).

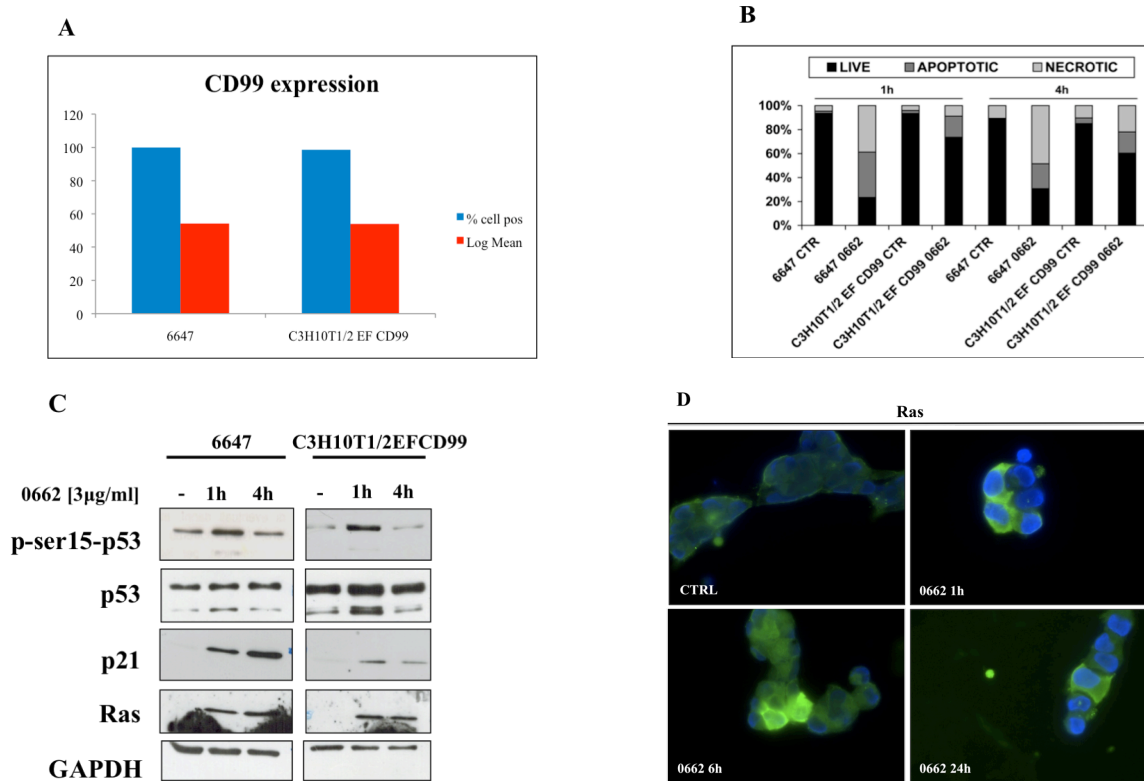


Figure 33. (A) FACS analysis of CD99 expression in 6647 (left) and in C3H10T1/2 EF CD99 (right). (B) Cell death evaluation by AnnexinV/PI binding in 6647 and in C3H10T1/2 EF CD99 with and without 0662 treatment (1h/4h). (C) Western blot analysis of p53 phosphorylation, p53 whole lysates, p21 and Ras upon 0662 mAb exposure (1h/4h). (D) IF assay showing Ras induction in C3H10T1/2 EF CD99 mAb-treated.

Conversely, when we silenced EWS/FLI1 we obtained a partial but significant reversal of the annexin-V positive cells after CD99 engagement (Figure 34). These

data were repeated in LAP35 (Figure 34) and, overall, they suggest that 0662 mAb preferentially delivers a massive cell death message in an aberrant cellular context in which both Ras upregulation and p53 reactivation are requested.

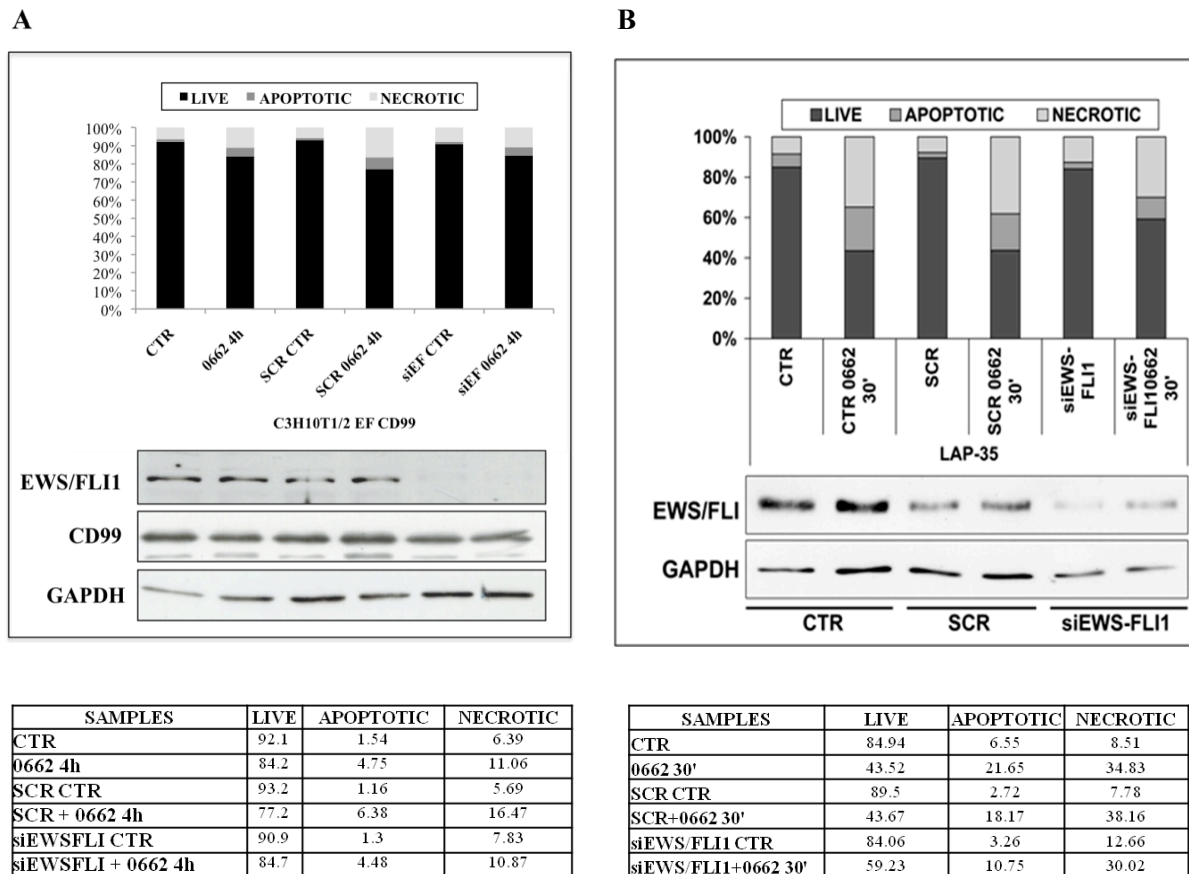


Figure 34. (A) Upper panel: histogram depicting Annexin V/PI positivity upon 0662 treatment on C3H10T1/2 EF CD99, and western blotting anti-EWS/FLI1 demonstrating the successful silencing. (B) Upper panel: evaluation of live, apoptotic and necrotic cells by annexin V/PI binding on LAP35 and western blot analysis showing the reliability of the silencing. In both lower panels values from respective histograms are reported.

DISCUSSION

Ewing Sarcoma is the second most common bone tumor after osteosarcoma; it is extremely rare and aggressive and characterized by a simple karyotype with a specific chromosomal rearrangement (the fusion of EWSR1 gene to a member of ETS family of transcription factors, most frequently FLI1), which leads to the formation of an aberrant fusion product responsible not only for the cell transformation itself but also for the maintenance of the disease (8, 9). Nevertheless, EWS/FLI1, despite its pivotal role as a driver of the malignancy, requires a permissive cellular background that includes an intact IGF pathway and the presence of CD99 molecule, essential elements without which it is not able to transform cells (40, 116). EWS/FLI1 promotes a high expression of CD99 in many cellular types (37, 39, 117), the latter a membrane glycoprotein involved in cellular adhesion mechanisms, apoptosis, T-cell and thymocytes differentiation (20, 29, 118), monocytes extravasation (119) and intracellular adhesion between lymphocytes and endothelial cells (120).

Because of its high expression on the Ewing cell surface, CD99 is considered to be a good marker for the diagnosis of the neoplasia (17, 23). Moreover, it was demonstrated the oncogenetic role of CD99 in ES cells, since it inhibits neural differentiation in this context (40). Molecular targeting by use of monoclonal antibodies has emerged as a new therapeutic strategy in many disorders. The CD99 is considered a selective and effective target for therapy of ES because it promotes homotypic aggregation and cancer cell death when triggered by specific antibodies (43, 44, 121). Although activation of the RAS/MAPK pathway in cancer cells is usually associated with tumor cell proliferation, recent studies support a paradoxical role in the initiation of cell death as well as in cell differentiation and growth arrest in specific cellular contexts, including ES (40, 71, 89, 94, 95). The tumor suppressor protein p53 is rarely mutated in ES (less than 10%) if compared to other malignancies, but is functionally inactivated by several mechanisms including

overexpression of MDM2(108, 122, 123). Both p53 and IGF-1R signaling are modulated as a consequence of MDM2 inactivation (109, 124). MDM2 is an E3 ubiquitin ligase that antagonizes the tumor suppressor p53 by inhibiting its ability to transactivate target genes or by promoting its degradation or nuclear export. Besides, MDM2 serves as a ubiquitin ligase for the IGF-1R, thereby causing its degradation by the proteasome (109-111). Preliminary data report a marked and rapid decrease of MDM2 protein levels following CD99 triggering; this downmodulation is both dose- and time-dependent and leads to p53 reactivation, thus contributing to CD99-induced caspase-independent cell death. As a consequence of MDM2 ubiquitination and proteasome-degradation, IGF-1R is upregulated following 0662 mAb treatments, leading, as a second step, to a decrease of IGF-1R levels on the cell surface because of the receptor internalization. At the same time, CD99 also undergoes an internalization process, both in a clathrin- and caveolin-1-dependent fashion, leading ultimately to a degradation of the receptor by lysosomes, predominantly; the degradation process is further validated by the lack of recycling of CD99 on the cell surface, since it fails to colocalize with Rab11, a late endosome marker involved in recycling processes. On the contrary, the demonstrated interaction with Rab4, an early endosome marker, proves that the entire mechanism takes place through the formation of endosomes, endocytic vesicles basically involved in the uptake of membrane proteins, lipids, extracellular ligands and soluble molecules, such as nutrients, from the cell surface into the cell interior.

CD99 and IGF-1R not only are internalized into the cell upon 0662 mAb employment, but they interact during the process; IF images and IP assays show that they are physically linked at the beginning of the process, forming a complex within endosomes, but later their fates are different: while CD99 undergoes a lysosome-mediated degradation, IGF-1R does not colocalize with Lamp-1, the main lysosome marker; this different sorting leads IGF-1R to a recycling on the cell surface again, keeping it active and able to emit signals. In this context we find Ras-MAPK pathway significantly upregulated; as mentioned in literature, RAS activation can induce non-

apoptotic cell death in neuroblastoma and in glioblastoma cells (71, 95). While in neuroblastoma cell death occurs through a classical autophagic process(95), in glioblastoma RAS acts through Rac-dependent pathways eventually hyperstimulating macropinocytosis (71). Since CD99-induced cell death is a caspase-independent mechanism (44), and electron microscopy images demonstrated that CD99 engagement induces a massive cytoplasm vacuolization, we investigated the role of autophagy in the observed mAb-induced death. Autophagic processes can either enhance cell survival in response to nutrient deprivation, organelle damage or stress, or result in cell death when sustained for a long time (68). Autophagy-associated cell death occurs without DNA fragmentation, nuclear collapse or cytoplasmic shrinkage and death is the result of excessive engulfment and subsequent digestion of proteins and organelles in response to cellular stresses (57). During this process, organelles and proteins are sequestered in a double-membrane vesicle called autophagosome. The formation of autophagosomes involves several specific proteins such as autophagy-related gene (Atg) 6 (Beclin-1) (125), the Atg12-Atg5-Atg16 complex and the ubiquitin-like protein Atg8 (known as LC3 in mammalian cells), which is activated by the Atg7 protein (125). The molecular marker of autophagy LC3, which is normally expressed in a diffuse pattern in healthy cells, was associated with vesicle membranes, and processed into its active LC3-IIIB form. Since silencing of Atg7, a crucial component of the autophagic machinery, was unable to rescue CD99-induced cell death, we concluded that ES cell death does not occur through autophagy as in neuroblastoma, but it happens with macropinocytosis followed by necrosis as in glioblastoma. We propose that RAS induction might contribute to the delivery of CD99-dependent death signals. Despite its well described role in tumorigenesis as a pro-survival/proliferation factor, increasing evidence indicates that RAS is able to switch cell fate toward death in specific cellular contexts, such as in normal primary cells (89) and in cancer cells under certain conditions (93). Indeed, we confirmed its involvement in favoring cell death by the employment of ES cell line expressing a Ras dominant negative construct, realizing a partial rescue from

death following 0662 treatments, if compared to that observed in parental cell line. Moreover, activation of RAS is required for mortality when cells are exposed to other inducers of cell death (126, 127). Accordingly, hMSCs expressing high levels of CD99 are insensitive to the 0662 mAb despite RAS induction, because no p53 reactivation occurs in these normal primary cells. RAS effects vary greatly in different cellular contexts and in relation to its expression level and cellular genetic context, switching from inducer of transformation in immortalized fibroblasts to driver of cell death in cancer cells or differentiation and growth arrest in neuronal, adipocytic, or myeloid cells (89). In this study we propose that in the non-transformed context of hMSCs the modest CD99-induced RAS upregulation is insufficient to commit cell towards cell death in absence of p53 cooperation. On the contrary, in cancer cells RAS continues to promote tumor growth, leaving them vulnerable to the effects of p53 reactivation and to the derived signaling conflict. We also determined that the presence of EWS/FLI1, which requires p53 inactivation for its oncogenic activity (128), sensitizes tumor cells to 0662 mAb; in fact, treatments carried out in the murine mesenchymal cell line double-transfected with CD99 and EWS/FLI1 (C3H10T1/2 EF CD99) resulted in a significant increase of cell death, with a concomitant phosphorylation of p53 and an induction of Ras stronger than that detected in hMSCs. Upon CD99 engagement and subsequent p53 reactivation, EWS/FLI1 activity becomes insufficient to sustain transformed ES cells. In this context, aberrant RAS up-regulation might deliver a death rather than a pro-survival signal. Concluding, we can depict the following scenario: CD99 triggering induces a rapid MDM2 ubiquitination and degradation. On one side, the abrogation of MDM2 reactivates p53 functions in ES cells, while on the other hand, the reported MDM2 downregulation causes the IGF-1R induction and its subsequent internalization inside endosomes with CD99 itself. Once internalized, IGF-1R is still able to signal and promotes a sustained activation of RAS, which may switch its functions from survival to cell death, in a context already pre-ordered by p53 activation. Unlike in healthy cells, engagement of CD99 in a EWS/FLI1-driven oncogenetic context

creates a synergy between RAS upregulation and p53 activation in ES cells, leading to cell death and thus allowing higher therapeutic selectivity.

REFERENCES

1. Helman LJ, Meltzer P. Mechanisms of sarcoma development. *Nat Rev Cancer*. 2003;3:685-94.
2. Lessnick SL, Ladanyi M. Molecular pathogenesis of Ewing sarcoma: new therapeutic and transcriptional targets. *Annu Rev Pathol*. 2012;7:145-59.
3. Manara MC, Garofalo C, Ferrari S, Belfiore A, Scotlandi K. Designing novel therapies against sarcomas in the era of personalized medicine and economic crisis. *Curr Pharm Des*. 2013;19:5344-61.
4. Bernstein M, Kovar H, Paulussen M, Randall RL, Schuck A, Teot LA, et al. Ewing's sarcoma family of tumors: current management. *Oncologist*. 2006;11:503-19.
5. Novakovic B, Goldstein AM, Wexler LH, Tucker MA. Increased risk of neuroectodermal tumors and stomach cancer in relatives of patients with Ewing's sarcoma family of tumors. *J Natl Cancer Inst*. 1994;86:1702-6.
6. Kim J, Pelletier J. Molecular genetics of chromosome translocations involving EWS and related family members. *Physiol Genomics*. 1999;1:127-38.
7. May WA, Lessnick SL, Braun BS, Klemsz M, Lewis BC, Lunsford LB, et al. The Ewing's sarcoma EWS/FLI-1 fusion gene encodes a more potent transcriptional activator and is a more powerful transforming gene than FLI-1. *Mol Cell Biol*. 1993;13:7393-8.
8. Ouchida M, Ohno T, Fujimura Y, Rao VN, Reddy ES. Loss of tumorigenicity of Ewing's sarcoma cells expressing antisense RNA to EWS-fusion transcripts. *Oncogene*. 1995;11:1049-54.
9. Maksimenko A, Malvy C. Oncogene-targeted antisense oligonucleotides for the treatment of Ewing sarcoma. *Expert Opin Ther Targets*. 2005;9:825-30.
10. Levy R, Dille J, Fox RI, Warnke R. A human thymus-leukemia antigen defined by hybridoma monoclonal antibodies. *Proc Natl Acad Sci U S A*. 1979;76:6552-6.
11. Goodfellow P, Pym B, Mohandas T, Shapiro LJ. The cell surface antigen locus, MIC2X, escapes X-inactivation. *Am J Hum Genet*. 1984;36:777-82.

12. Aubrit F, Gelin C, Pham D, Raynal B, Bernard A. The biochemical characterization of E2, a T cell surface molecule involved in rosettes. *Eur J Immunol.* 1989;19:1431-6.
13. Banting GS, Pym B, Darling SM, Goodfellow PN. The MIC2 gene product: epitope mapping and structural prediction analysis define an integral membrane protein. *Mol Immunol.* 1989;26:181-8.
14. Gelin C, Aubrit F, Phalipon A, Raynal B, Cole S, Kaczorek M, et al. The E2 antigen, a 32 kd glycoprotein involved in T-cell adhesion processes, is the MIC2 gene product. *EMBO J.* 1989;8:3253-9.
15. Goodfellow PJ, Darling SM, Thomas NS, Goodfellow PN. A pseudoautosomal gene in man. *Science.* 1986;234:740-3.
16. Kim HY, Kim YM, Shin YK, Park SH, Lee W. Solution structure of the cytoplasmic domain of human CD99 type I. *Mol Cells.* 2004;18:24-9.
17. Ambros IM, Ambros PF, Strehl S, Kovar H, Gadner H, Salzer-Kuntschik M. MIC2 is a specific marker for Ewing's sarcoma and peripheral primitive neuroectodermal tumors. Evidence for a common histogenesis of Ewing's sarcoma and peripheral primitive neuroectodermal tumors from MIC2 expression and specific chromosome aberration. *Cancer.* 1991;67:1886-93.
18. Dworzak MN, Fritsch G, Buchinger P, Fleischer C, Printz D, Zellner A, et al. Flow cytometric assessment of human MIC2 expression in bone marrow, thymus, and peripheral blood. *Blood.* 1994;83:415-25.
19. Choi EY, Park WS, Jung KC, Kim SH, Kim YY, Lee WJ, et al. Engagement of CD99 induces up-regulation of TCR and MHC class I and II molecules on the surface of human thymocytes. *J Immunol.* 1998;161:749-54.
20. Bernard G, Zoccola D, Deckert M, Breittmayer JP, Aussel C, Bernard A. The E2 molecule (CD99) specifically triggers homotypic aggregation of CD4+ CD8+ thymocytes. *J Immunol.* 1995;154:26-32.
21. Gelin C, Zoccola D, Valentin H, Raynal B, Bernard A. Isoforms of the E2 molecule: D44 monoclonal antibody defines an epitope on E2 and reacts differentially with T cell subsets. *Eur J Immunol.* 1991;21:715-9.
22. Ramani P, Rampling D, Link M. Immunocytochemical study of 12E7 in small round-cell tumours of childhood: an assessment of its sensitivity and specificity. *Histopathology.* 1993;23:557-61.

23. Kovar H, Dworzak M, Strehl S, Schnell E, Ambros IM, Ambros PF, et al. Overexpression of the pseudoautosomal gene MIC2 in Ewing's sarcoma and peripheral primitive neuroectodermal tumor. *Oncogene*. 1990;5:1067-70.
24. Fisher C. Synovial sarcoma. *Ann Diagn Pathol*. 1998;2:401-21.
25. Granter SR, Renshaw AA, Fletcher CD, Bhan AK, Rosenberg AE. CD99 reactivity in mesenchymal chondrosarcoma. *Hum Pathol*. 1996;27:1273-6.
26. Brown RE, Boyle JL. Mesenchymal chondrosarcoma: molecular characterization by a proteomic approach, with morphogenic and therapeutic implications. *Ann Clin Lab Sci*. 2003;33:131-41.
27. Mahfouz S, Aziz AA, Gabal SM, el-Sheikh S. Immunohistochemical study of CD99 and EMA expression in ependymomas. *Medscape J Med*. 2008;10:41.
28. Lou O, Alcaide P, Luscinskas FW, Muller WA. CD99 is a key mediator of the transendothelial migration of neutrophils. *J Immunol*. 2007;178:1136-43.
29. Bernard G, Breitmayer JP, de Matteis M, Trampont P, Hofman P, Senik A, et al. Apoptosis of immature thymocytes mediated by E2/CD99. *J Immunol*. 1997;158:2543-50.
30. Sohn HW, Shin YK, Lee IS, Bae YM, Suh YH, Kim MK, et al. CD99 regulates the transport of MHC class I molecules from the Golgi complex to the cell surface. *J Immunol*. 2001;166:787-94.
31. Bremond A, Meynet O, Mahiddine K, Coito S, Tichet M, Scotlandi K, et al. Regulation of HLA class I surface expression requires CD99 and p230/golgin-245 interaction. *Blood*. 2009;113:347-57.
32. Dworzak MN, Froschl G, Printz D, Zen LD, Gaipa G, Ratei R, et al. CD99 expression in T-lineage ALL: implications for flow cytometric detection of minimal residual disease. *Leukemia*. 2004;18:703-8.
33. Rajaram V, Brat DJ, Perry A. Anaplastic meningioma versus meningeal hemangiopericytoma: immunohistochemical and genetic markers. *Hum Pathol*. 2004;35:1413-8.
34. Seol HJ, Chang JH, Yamamoto J, Romagnuolo R, Suh Y, Weeks A, et al. Overexpression of CD99 Increases the Migration and Invasiveness of Human Malignant Glioma Cells. *Genes Cancer*. 2012;3:535-49.

35. Manara MC, Bernard G, Lollini PL, Nanni P, Zuntini M, Landuzzi L, et al. CD99 acts as an oncosuppressor in osteosarcoma. *Mol Biol Cell*. 2006;17:1910-21.
36. Scotlandi K, Zuntini M, Manara MC, Sciandra M, Rocchi A, Benini S, et al. CD99 isoforms dictate opposite functions in tumour malignancy and metastases by activating or repressing c-Src kinase activity. *Oncogene*. 2007;26:6604-18.
37. Miyagawa Y, Okita H, Nakajima H, Horiuchi Y, Sato B, Taguchi T, et al. Inducible expression of chimeric EWS/ETS proteins confers Ewing's family tumor-like phenotypes to human mesenchymal progenitor cells. *Mol Cell Biol*. 2008;28:2125-37.
38. Riggi N, Suva ML, Suva D, Cironi L, Provero P, Tercier S, et al. EWS-FLI-1 expression triggers a Ewing's sarcoma initiation program in primary human mesenchymal stem cells. *Cancer Res*. 2008;68:2176-85.
39. Hu-Lieskovan S, Zhang J, Wu L, Shimada H, Schofield DE, Triche TJ. EWS-FLI1 fusion protein up-regulates critical genes in neural crest development and is responsible for the observed phenotype of Ewing's family of tumors. *Cancer Res*. 2005;65:4633-44.
40. Rocchi A, Manara MC, Sciandra M, Zambelli D, Nardi F, Nicoletti G, et al. CD99 inhibits neural differentiation of human Ewing sarcoma cells and thereby contributes to oncogenesis. *J Clin Invest*. 2010;120:668-80.
41. Franzetti GA, Laud-Duval K, Bellanger D, Stern MH, Sastre-Garau X, Delattre O. MiR-30a-5p connects EWS-FLI1 and CD99, two major therapeutic targets in Ewing tumor. *Oncogene*. 2013;32:3915-21.
42. Jung KC, Kim NH, Park WS, Park SH, Bae Y. The CD99 signal enhances Fas-mediated apoptosis in the human leukemic cell line, Jurkat. *FEBS Lett*. 2003;554:478-84.
43. Scotlandi K, Baldini N, Cerisano V, Manara MC, Benini S, Serra M, et al. CD99 engagement: an effective therapeutic strategy for Ewing tumors. *Cancer Res*. 2000;60:5134-42.
44. Cerisano V, Aalto Y, Perdichizzi S, Bernard G, Manara MC, Benini S, et al. Molecular mechanisms of CD99-induced caspase-independent cell death and cell-cell adhesion in Ewing's sarcoma cells: actin and zyxin as key intracellular mediators. *Oncogene*. 2004;23:5664-74.

45. Scotlandi K, Perdichizzi S, Bernard G, Nicoletti G, Nanni P, Lollini PL, et al. Targeting CD99 in association with doxorubicin: an effective combined treatment for Ewing's sarcoma. *Eur J Cancer*. 2006;42:91-6.
46. Llombart-Bosch A, Machado I, Navarro S, Bertoni F, Bacchini P, Alberghini M, et al. Histological heterogeneity of Ewing's sarcoma/PNET: an immunohistochemical analysis of 415 genetically confirmed cases with clinical support. *Virchows Arch*. 2009;455:397-411.
47. Melino G. The Sirens' song. *Nature*. 2001;412:23.
48. Kroemer G, El-Deiry WS, Golstein P, Peter ME, Vaux D, Vandenabeele P, et al. Classification of cell death: recommendations of the Nomenclature Committee on Cell Death. *Cell Death Differ*. 2005;12 Suppl 2:1463-7.
49. Cohen GM. Caspases: the executioners of apoptosis. *Biochem J*. 1997;326 (Pt 1):1-16.
50. Green D, Kroemer G. The central executioners of apoptosis: caspases or mitochondria? *Trends Cell Biol*. 1998;8:267-71.
51. Green DR, Kroemer G. The pathophysiology of mitochondrial cell death. *Science*. 2004;305:626-9.
52. Kroemer G, Galluzzi L, Vandenabeele P, Abrams J, Alnemri ES, Baehrecke EH, et al. Classification of cell death: recommendations of the Nomenclature Committee on Cell Death 2009. *Cell Death Differ*. 2009;16:3-11.
53. Kerr JF, Wyllie AH, Currie AR. Apoptosis: a basic biological phenomenon with wide-ranging implications in tissue kinetics. *Br J Cancer*. 1972;26:239-57.
54. Chipuk JE, Green DR. Dissecting p53-dependent apoptosis. *Cell Death Differ*. 2006;13:994-1002.
55. Li P, Nijhawan D, Budihardjo I, Srinivasula SM, Ahmad M, Alnemri ES, et al. Cytochrome c and dATP-dependent formation of Apaf-1/caspase-9 complex initiates an apoptotic protease cascade. *Cell*. 1997;91:479-89.
56. Goldstein JC, Munoz-Pinedo C, Ricci JE, Adams SR, Kelekar A, Schuler M, et al. Cytochrome c is released in a single step during apoptosis. *Cell Death Differ*. 2005;12:453-62.
57. Hotchkiss RS, Strasser A, McDunn JE, Swanson PE. Cell death. *N Engl J Med*. 2009;361:1570-83.

58. Klionsky DJ, Abeliovich H, Agostinis P, Agrawal DK, Aliev G, Askew DS, et al. Guidelines for the use and interpretation of assays for monitoring autophagy in higher eukaryotes. *Autophagy*. 2008;4:151-75.
59. Levine B, Deretic V. Unveiling the roles of autophagy in innate and adaptive immunity. *Nat Rev Immunol*. 2007;7:767-77.
60. Clarke PG. Developmental cell death: morphological diversity and multiple mechanisms. *Anat Embryol (Berl)*. 1990;181:195-213.
61. Baehrecke EH. Autophagy: dual roles in life and death? *Nat Rev Mol Cell Biol*. 2005;6:505-10.
62. Levine B, Klionsky DJ. Development by self-digestion: molecular mechanisms and biological functions of autophagy. *Dev Cell*. 2004;6:463-77.
63. Levine B, Kroemer G. Autophagy in the pathogenesis of disease. *Cell*. 2008;132:27-42.
64. Simonsen A, Tooze SA. Coordination of membrane events during autophagy by multiple class III PI3-kinase complexes. *J Cell Biol*. 2009;186:773-82.
65. Geng J, Klionsky DJ. The Atg8 and Atg12 ubiquitin-like conjugation systems in macroautophagy. 'Protein modifications: beyond the usual suspects' review series. *EMBO Rep*. 2008;9:859-64.
66. Hanada T, Noda NN, Satomi Y, Ichimura Y, Fujioka Y, Takao T, et al. The Atg12-Atg5 conjugate has a novel E3-like activity for protein lipidation in autophagy. *J Biol Chem*. 2007;282:37298-302.
67. Fujita N, Itoh T, Omori H, Fukuda M, Noda T, Yoshimori T. The Atg16L complex specifies the site of LC3 lipidation for membrane biogenesis in autophagy. *Mol Biol Cell*. 2008;19:2092-100.
68. Kimmelman AC. The dynamic nature of autophagy in cancer. *Genes Dev*. 2011;25:1999-2010.
69. Lockshin RA, Zakeri Z. Apoptosis, autophagy, and more. *Int J Biochem Cell Biol*. 2004;36:2405-19.
70. Chi S, Kitanaka C, Noguchi K, Mochizuki T, Nagashima Y, Shirouzu M, et al. Oncogenic Ras triggers cell suicide through the activation of a caspase-independent cell death program in human cancer cells. *Oncogene*. 1999;18:2281-90.

71. Overmeyer JH, Kaul A, Johnson EE, Maltese WA. Active ras triggers death in glioblastoma cells through hyperstimulation of macropinocytosis. *Mol Cancer Res.* 2008;6:965-77.
72. Lim JP, Gleeson PA. Macropinocytosis: an endocytic pathway for internalising large gulps. *Immunol Cell Biol.* 2011;89:836-43.
73. Carpentier JL, Lew DP, Paccaud JP, Gil R, Iacopetta B, Kazatchkine M, et al. Internalization pathway of C3b receptors in human neutrophils and its transmodulation by chemoattractant receptors stimulation. *Cell Regul.* 1991;2:41-55.
74. Sallusto F, Cella M, Danieli C, Lanzavecchia A. Dendritic cells use macropinocytosis and the mannose receptor to concentrate macromolecules in the major histocompatibility complex class II compartment: downregulation by cytokines and bacterial products. *J Exp Med.* 1995;182:389-400.
75. Norbury CC, Chambers BJ, Prescott AR, Ljunggren HG, Watts C. Constitutive macropinocytosis allows TAP-dependent major histocompatibility complex class I presentation of exogenous soluble antigen by bone marrow-derived dendritic cells. *Eur J Immunol.* 1997;27:280-8.
76. Hacker U, Albrecht R, Maniak M. Fluid-phase uptake by macropinocytosis in *Dictyostelium*. *J Cell Sci.* 1997;110 (Pt 2):105-12.
77. Araki N, Hatae T, Yamada T, Hirohashi S. Actinin-4 is preferentially involved in circular ruffling and macropinocytosis in mouse macrophages: analysis by fluorescence ratio imaging. *J Cell Sci.* 2000;113 (Pt 18):3329-40.
78. Tollefsen SE, Stoszek RM, Thompson K. Interaction of the alpha beta dimers of the insulin-like growth factor I receptor is required for receptor autophosphorylation. *Biochemistry.* 1991;30:48-54.
79. Kato H, Faria TN, Stannard B, Roberts CT, Jr., LeRoith D. Role of tyrosine kinase activity in signal transduction by the insulin-like growth factor-I (IGF-I) receptor. Characterization of kinase-deficient IGF-I receptors and the action of an IGF-I-mimetic antibody (alpha IR-3). *J Biol Chem.* 1993;268:2655-61.
80. Ravichandran KS. Signaling via Shc family adapter proteins. *Oncogene.* 2001;20:6322-30.
81. Zha J, Lackner MR. Targeting the insulin-like growth factor receptor-1R pathway for cancer therapy. *Clin Cancer Res.* 2010;16:2512-7.

82. Matsumoto K, Asano T, Endo T. Novel small GTPase M-Ras participates in reorganization of actin cytoskeleton. *Oncogene*. 1997;15:2409-17.
83. Lowy DR, Willumsen BM. Function and regulation of ras. *Annu Rev Biochem*. 1993;62:851-91.
84. Wittinghofer A, Pai EF. The structure of Ras protein: a model for a universal molecular switch. *Trends Biochem Sci*. 1991;16:382-7.
85. Barbacid M. ras genes. *Annu Rev Biochem*. 1987;56:779-827.
86. Ma J, Karplus M. Molecular switch in signal transduction: reaction paths of the conformational changes in ras p21. *Proc Natl Acad Sci U S A*. 1997;94:11905-10.
87. Polakis P, McCormick F. Structural requirements for the interaction of p21ras with GAP, exchange factors, and its biological effector target. *J Biol Chem*. 1993;268:9157-60.
88. Jurnak F. The three-dimensional structure of c-H-ras p21: implications for oncogene and G protein studies. *Trends Biochem Sci*. 1988;13:195-8.
89. Crespo P, Leon J. Ras proteins in the control of the cell cycle and cell differentiation. *Cell Mol Life Sci*. 2000;57:1613-36.
90. Sperandio S, de Belle I, Bredesen DE. An alternative, nonapoptotic form of programmed cell death. *Proc Natl Acad Sci U S A*. 2000;97:14376-81.
91. Sperandio S, Poksay K, de Belle I, Lafuente MJ, Liu B, Nasir J, et al. Paraptosis: mediation by MAP kinases and inhibition by AIP-1/Alix. *Cell Death Differ*. 2004;11:1066-75.
92. Boucher J, Macotela Y, Bezy O, Mori MA, Kriauciunas K, Kahn CR. A kinase-independent role for unoccupied insulin and IGF-1 receptors in the control of apoptosis. *Sci Signal*. 2010;3:ra87.
93. Overmeyer JH, Maltese WA. Death pathways triggered by activated Ras in cancer cells. *Front Biosci (Landmark Ed)*. 2011;16:1693-713.
94. Elgendy M, Sheridan C, Brumatti G, Martin SJ. Oncogenic Ras-induced expression of Noxa and Beclin-1 promotes autophagic cell death and limits clonogenic survival. *Mol Cell*. 2011;42:23-35.
95. Chin L, Tam A, Pomerantz J, Wong M, Holash J, Bardeesy N, et al. Essential role for oncogenic Ras in tumour maintenance. *Nature*. 1999;400:468-72.

96. Murphy LO, Blenis J. MAPK signal specificity: the right place at the right time. *Trends Biochem Sci.* 2006;31:268-75.
97. Cagnol S, Van Obberghen-Schilling E, Chambard JC. Prolonged activation of ERK1,2 induces FADD-independent caspase 8 activation and cell death. *Apoptosis.* 2006;11:337-46.
98. Wang X, Martindale JL, Holbrook NJ. Requirement for ERK activation in cisplatin-induced apoptosis. *J Biol Chem.* 2000;275:39435-43.
99. Zhang CL, Wu LJ, Zuo HJ, Tashiro S, Onodera S, Ikejima T. Cytochrome c release from oridonin-treated apoptotic A375-S2 cells is dependent on p53 and extracellular signal-regulated kinase activation. *J Pharmacol Sci.* 2004;96:155-63.
100. Kim GS, Hong JS, Kim SW, Koh JM, An CS, Choi JY, et al. Leptin induces apoptosis via ERK/cPLA2/cytochrome c pathway in human bone marrow stromal cells. *J Biol Chem.* 2003;278:21920-9.
101. Schweyer S, Soruri A, Meschter O, Heintze A, Zschunke F, Miosge N, et al. Cisplatin-induced apoptosis in human malignant testicular germ cell lines depends on MEK/ERK activation. *Br J Cancer.* 2004;91:589-98.
102. Nesterov A, Nikrad M, Johnson T, Kraft AS. Oncogenic Ras sensitizes normal human cells to tumor necrosis factor-alpha-related apoptosis-inducing ligand-induced apoptosis. *Cancer Res.* 2004;64:3922-7.
103. Cheng Y, Qiu F, Tashiro S, Onodera S, Ikejima T. ERK and JNK mediate TNFalpha-induced p53 activation in apoptotic and autophagic L929 cell death. *Biochem Biophys Res Commun.* 2008;376:483-8.
104. Liu J, Mao W, Ding B, Liang CS. ERKs/p53 signal transduction pathway is involved in doxorubicin-induced apoptosis in H9c2 cells and cardiomyocytes. *Am J Physiol Heart Circ Physiol.* 2008;295:H1956-65.
105. Shih A, Davis FB, Lin HY, Davis PJ. Resveratrol induces apoptosis in thyroid cancer cell lines via a MAPK- and p53-dependent mechanism. *J Clin Endocrinol Metab.* 2002;87:1223-32.
106. Lin T, Mak NK, Yang MS. MAPK regulate p53-dependent cell death induced by benzo[a]pyrene: involvement of p53 phosphorylation and acetylation. *Toxicology.* 2008;247:145-53.

107. Courtois-Cox S, Genter Williams SM, Reczek EE, Johnson BW, McGillicuddy LT, Johannessen CM, et al. A negative feedback signaling network underlies oncogene-induced senescence. *Cancer Cell*. 2006;10:459-72.
108. Ladanyi M, Lewis R, Jhanwar SC, Gerald W, Huvos AG, Healey JH. MDM2 and CDK4 gene amplification in Ewing's sarcoma. *J Pathol*. 1995;175:211-7.
109. Girnita L, Girnita A, Larsson O. Mdm2-dependent ubiquitination and degradation of the insulin-like growth factor 1 receptor. *Proc Natl Acad Sci U S A*. 2003;100:8247-52.
110. Larsson O, Girnita A, Girnita L. Role of insulin-like growth factor 1 receptor signalling in cancer. *Br J Cancer*. 2005;92:2097-101.
111. Froment P, Dupont J, Christophe-Marine J. Mdm2 exerts pro-apoptotic activities by antagonizing insulin-like growth factor-I-mediated survival. *Cell Cycle*. 2008;7:3098-103.
112. Fehrenbacher N, Bar-Sagi D, Philips M. Ras/MAPK signaling from endomembranes. *Mol Oncol*. 2009;3:297-307.
113. Prior IA, Hancock JF. Ras trafficking, localization and compartmentalized signalling. *Semin Cell Dev Biol*. 2012;23:145-53.
114. Barth JM, Szabad J, Hafen E, Kohler K. Autophagy in *Drosophila* ovaries is induced by starvation and is required for oogenesis. *Cell Death Differ*. 2011;18:915-24.
115. Matallanas D, Arozarena I, Berciano MT, Aaronson DS, Pellicer A, Lafarga M, et al. Differences on the inhibitory specificities of H-Ras, K-Ras, and N-Ras (N17) dominant negative mutants are related to their membrane microlocalization. *J Biol Chem*. 2003;278:4572-81.
116. Toretsky JA, Kalebic T, Blakesley V, LeRoith D, Helman LJ. The insulin-like growth factor-I receptor is required for EWS/FLI-1 transformation of fibroblasts. *J Biol Chem*. 1997;272:30822-7.
117. Lessnick SL, Dacwag CS, Golub TR. The Ewing's sarcoma oncoprotein EWS/FLI induces a p53-dependent growth arrest in primary human fibroblasts. *Cancer Cell*. 2002;1:393-401.
118. Alberti I, Bernard G, Rouquette-Jazdanian AK, Pelassy C, Pourtejn M, Aussel C, et al. CD99 isoforms expression dictates T cell functional outcomes. *FASEB J*. 2002;16:1946-8.

119. Schenkel AR, Mamdouh Z, Chen X, Liebman RM, Muller WA. CD99 plays a major role in the migration of monocytes through endothelial junctions. *Nat Immunol.* 2002;3:143-50.
120. Bernard G, Raimondi V, Alberti I, Pourtein M, Widjenes J, Ticchioni M, et al. CD99 (E2) up-regulates alpha4beta1-dependent T cell adhesion to inflamed vascular endothelium under flow conditions. *Eur J Immunol.* 2000;30:3061-5.
121. Sohn HW, Choi EY, Kim SH, Lee IS, Chung DH, Sung UA, et al. Engagement of CD99 induces apoptosis through a calcineurin-independent pathway in Ewing's sarcoma cells. *Am J Pathol.* 1998;153:1937-45.
122. Ottaviano L, Schaefer KL, Gajewski M, Huckenbeck W, Baldus S, Rogel U, et al. Molecular characterization of commonly used cell lines for bone tumor research: a trans-European EuroBoNet effort. *Genes Chromosomes Cancer.* 2010;49:40-51.
123. Neilsen PM, Pishas KI, Callen DF, Thomas DM. Targeting the p53 Pathway in Ewing Sarcoma. *Sarcoma.* 2011;2011:746939.
124. Kubbutat MH, Jones SN, Vousden KH. Regulation of p53 stability by Mdm2. *Nature.* 1997;387:299-303.
125. Tsujimoto Y, Shimizu S. Another way to die: autophagic programmed cell death. *Cell Death Differ.* 2005;12 Suppl 2:1528-34.
126. Suzuki J, Kaziro Y, Koide H. An activated mutant of R-Ras inhibits cell death caused by cytokine deprivation in BaF3 cells in the presence of IGF-I. *Oncogene.* 1997;15:1689-97.
127. Gulbins E, Brenner B, Koppenhoefer U, Linderkamp O, Lang F. Fas or ceramide induce apoptosis by Ras-regulated phosphoinositide-3-kinase activation. *J Leukoc Biol.* 1998;63:253-63.
128. Deneen B, Denny CT. Loss of p16 pathways stabilizes EWS/FLI1 expression and complements EWS/FLI1 mediated transformation. *Oncogene.* 2001;20:6731-41.